Dr. Remeis-Sternwarte Bamberg
Astronomical Institute of the
University of Erlangen-Nuremberg

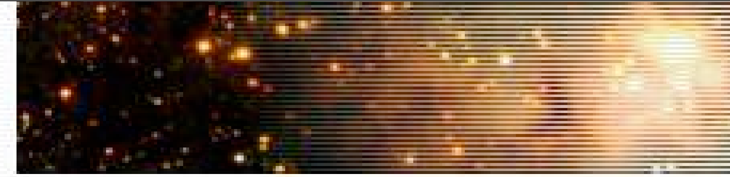

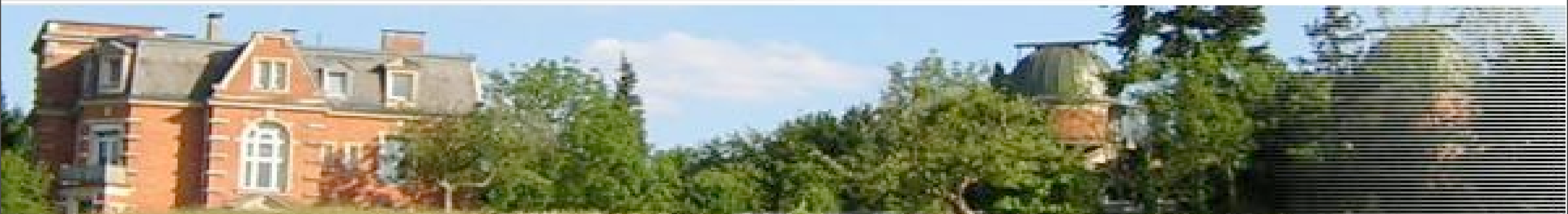

Stellar Parameter Determination

Standard Methods & NLTE Refinements

N. Przybilla & M.F. Nieva

Requirements for accurate analyses

- local temperature & particle densities need to be known

  ➡ atmospheric structure

- radiation field realistic

  ➡ $S_\nu \neq B_\nu(T)$

atmospheric parameters

- all relevant processes taken into account for SE

- high-quality atomic data available

  ➡ ab-initio calculations

➡ any weakness affects overall accuracy

Why accurate analyses?

understand stars across HRD

- stellar atmospheres
- stellar structure
- stellar evolution
- nucleosynthesis
- cosmic cycle of matter
- galactic evolution
- cosmology
- . . .

Diagnostic Problem

stellar analyses from
interpretation of observation

→ photometry, spectroscopy

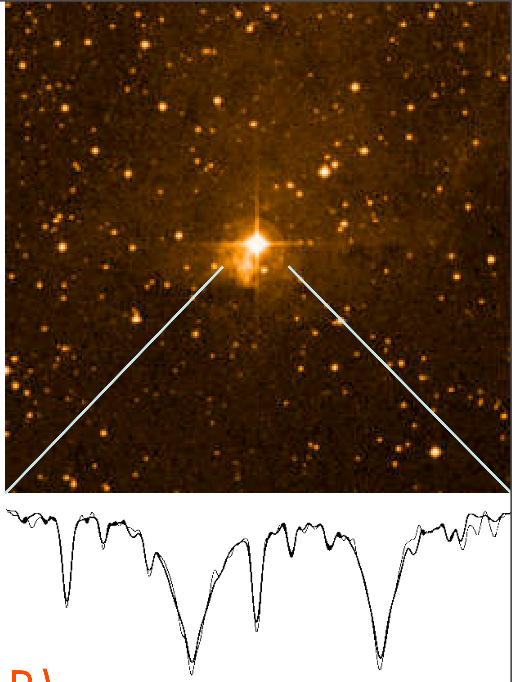

- fundamental physical properties: M, L, R   (Ω, B)
  → direct methods only for few stars
- atmospheric parameters: T_{eff}, log *g*, ξ, Y, Z, ...
- chemical composition

→ quantitative spectroscopy
via model atmospheres

Fundamental determinations of stellar parameters

- from detached eclipsing binary systems → M, R
- for standard stars:
  - Sun
  - Vega
  - Procyon
  - Arcturus
  - & a few other ...

Characterisation of a Star
Praxis

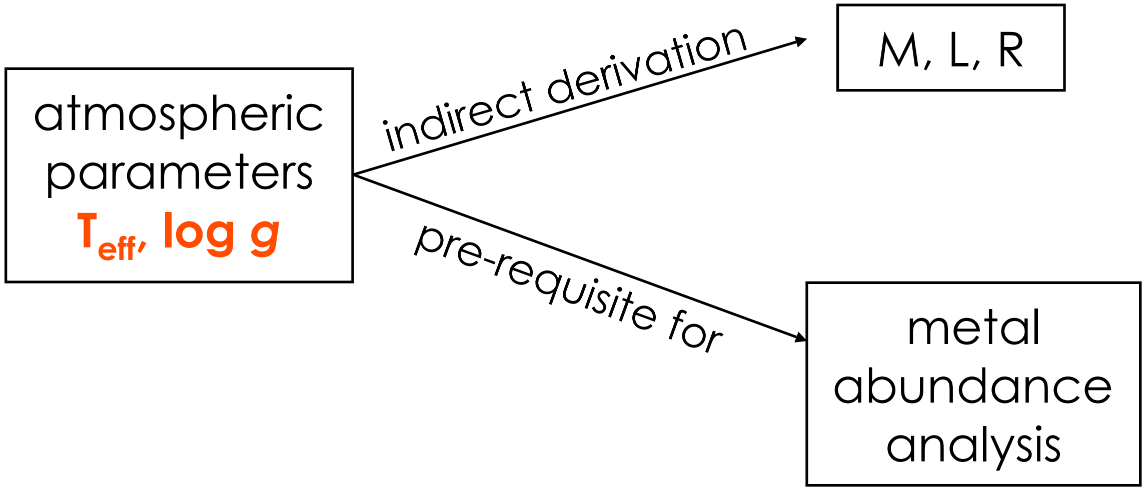

T_{eff} & log g: - define physical conditions of stellar atmosphere

also: microturbulence, global metallicity, H & He abundance

➡ T & P-stratification

Atmospheric Parameter Determination

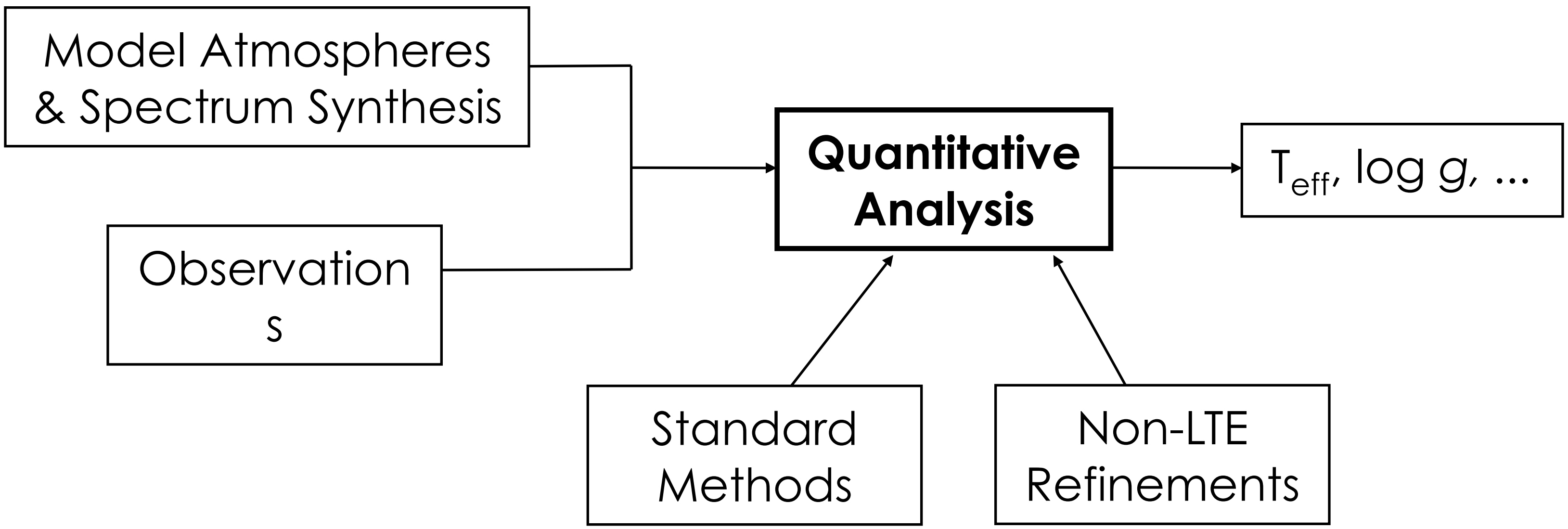

Photometric Techniques

Photometry

- idea: sample stellar flux distribution by a few bandpasses
- observationally'cheap': easy to obtain for large numbers of objects
- availability of large amounts of data:
  - broadband: e.g. Johnson
  - smallband: e.g. Strömgren
  - IR: e.g. 2MASS
- calibrated on basis of line-blanketed LTE model atmospheres
- highly useful for analysis of large stellar samples
- accuracy: ~1... x%

Smallband photometry: e.g. Strömgren

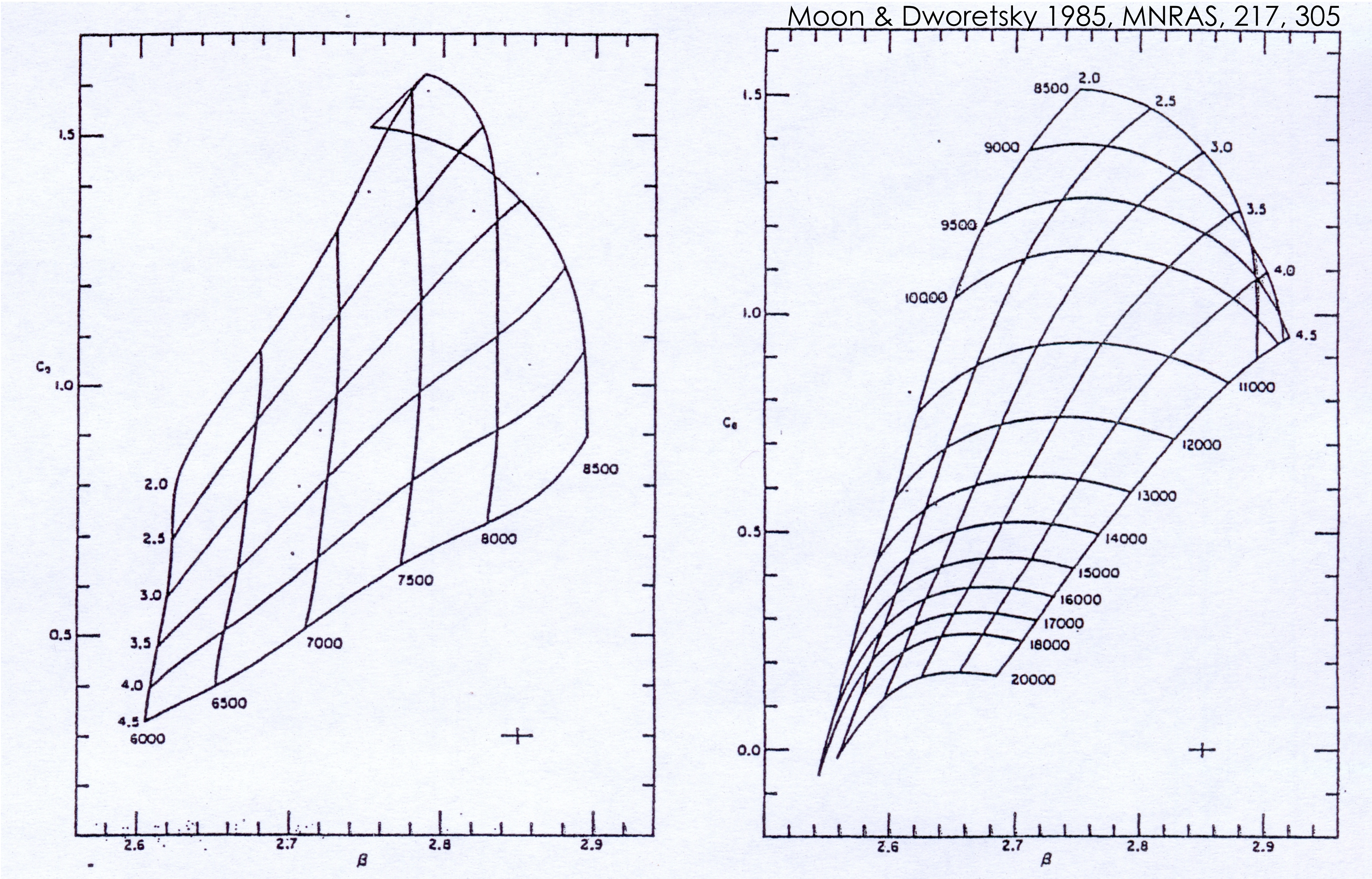

- comparison of different calibrations by Napiwotzki et al. 1993, A&A, 268, 653

unconfortable disagreement → improvements

Broadband photometry: e.g. Johnson

Daflon et al. 1999, ApJ, 522, 950

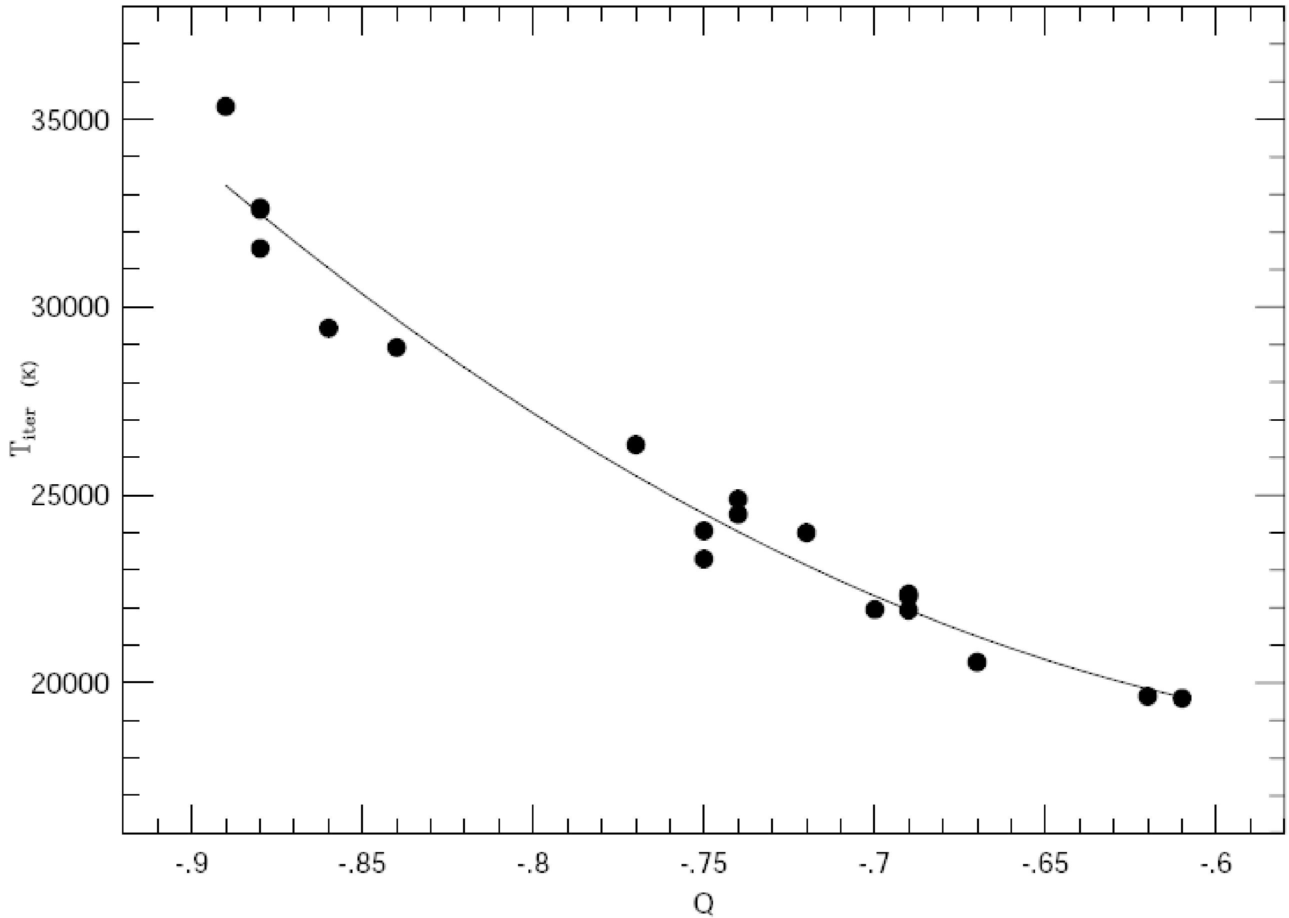

Q=(U-B)-0.72(B-V)   - reddening free

Comparison of different T_{eff}-indicators in B stars

Poster by M.I. Zavallos Herencia & S. Daflon

	T_Q	T_L	T_S	T_{S-N}	T_{Si-LTE}	$T_{Si-NLTE}$	$\varepsilon(O\ II)_{LTE}$
NGC2244-376	30010	27650	33900	29410	32950	-	8.33 ... 8.83
NGC2244-201	29670	27380	27260	27170	27800	28300	8.76 ... 8.81

→ $\Delta T > 5000K$ possible

line-to-line scatter: 1σ(abundance): ~0.1 ... ~0.5dex

Spectrophotometry

- ground-based spectrophotometry highly useful

Adelman et al. 2002, A&A, 392, 1031

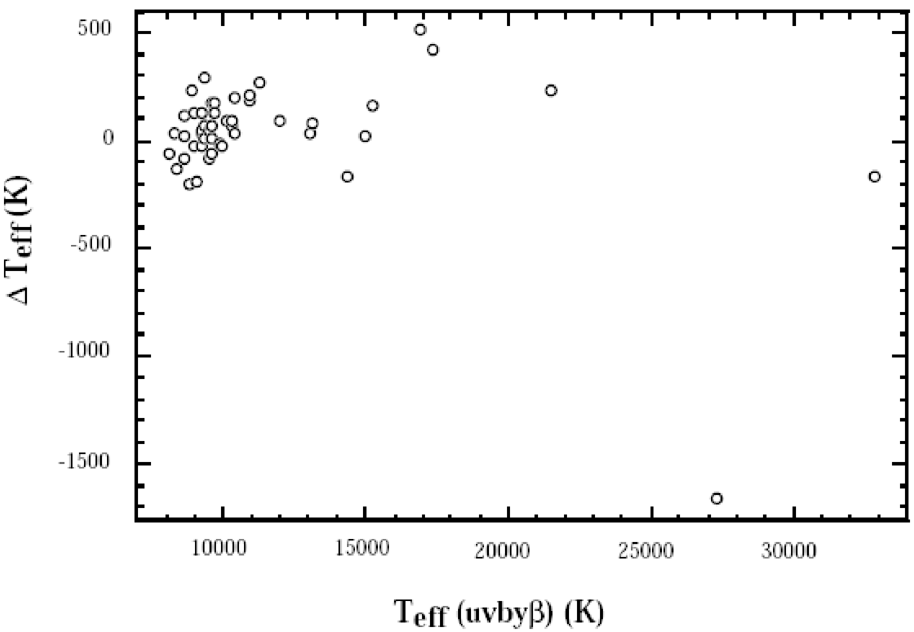

Fig. 5. The differences ($\Delta T_{\rm eff}$ (K)) (photometric minus spectrophotometric-Hγ values) of the effective temperatures as a function of the photometric temperature $T_{\rm eff}$ $(uvby\beta)$ (K).

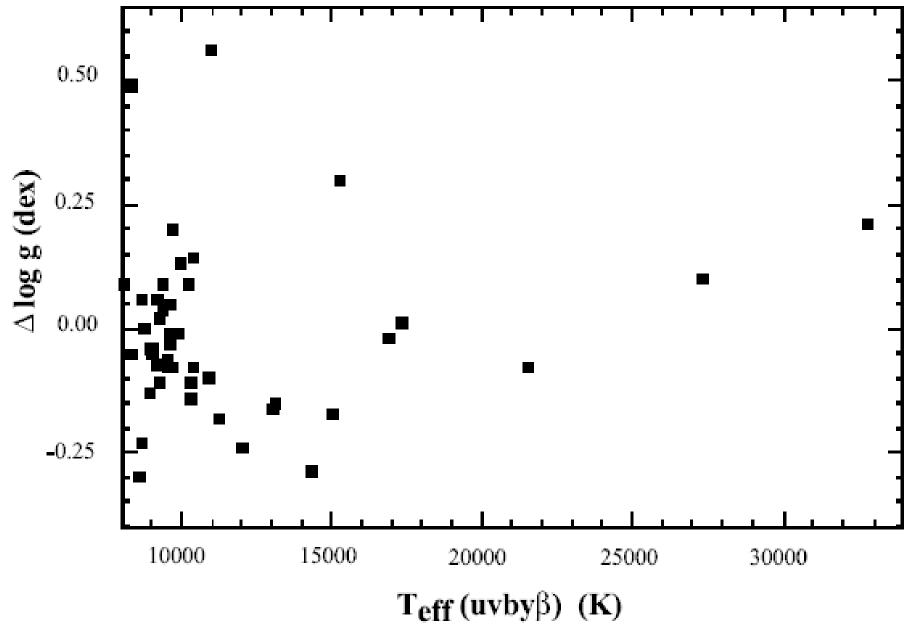

Fig. 6. The differences ($\Delta \log g$ (dex)) (photometric minus spectrophotometric-Hγ values) of the surface gravities as a function of the photometric temperature $T_{\rm eff}$ $(uvby\beta)$ (K).

- flux-calibrated data in UV : IUE, HST, FUSE, ... → hot stars

Other methods:

- IRFM
- T_{eff}- colour relations
- spectral type – T_{eff} relations
- line ratios
- excitation temperatures

Spectroscopic Techniques

Kurucz 1979, ApJS, 40, 1

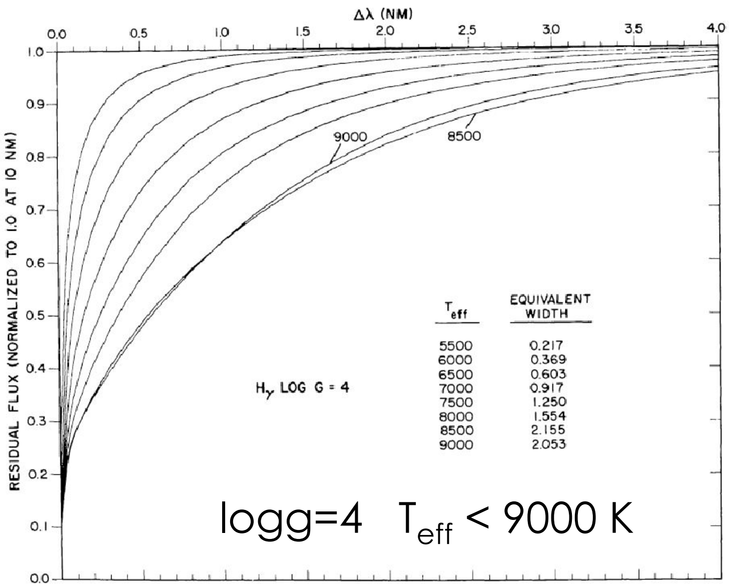

FIG. 21.—Hγ profiles for solar abundance models with $T_{eff} \leq 9000$ K. Equivalent widths are given in nm.

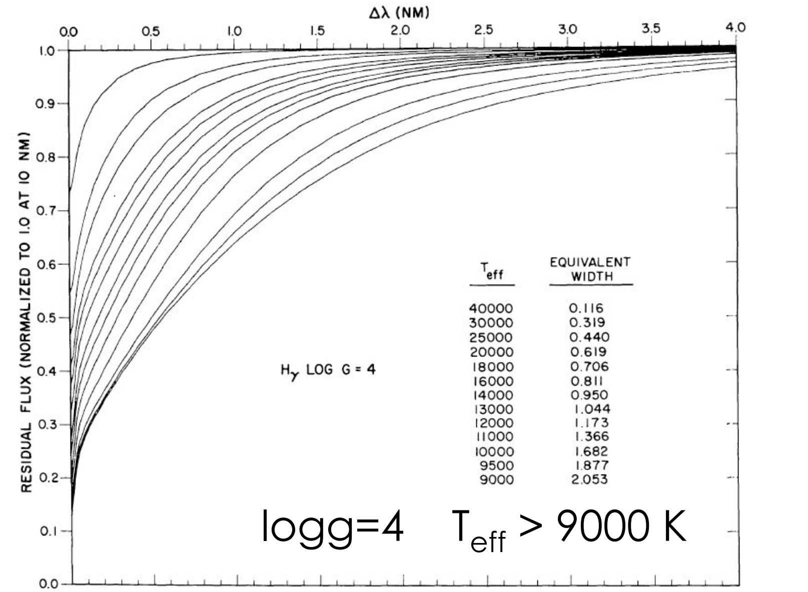

FIG. 23.—Hγ profiles for the early-type models showing the decrease in equivalent width with increasing T_{eff}

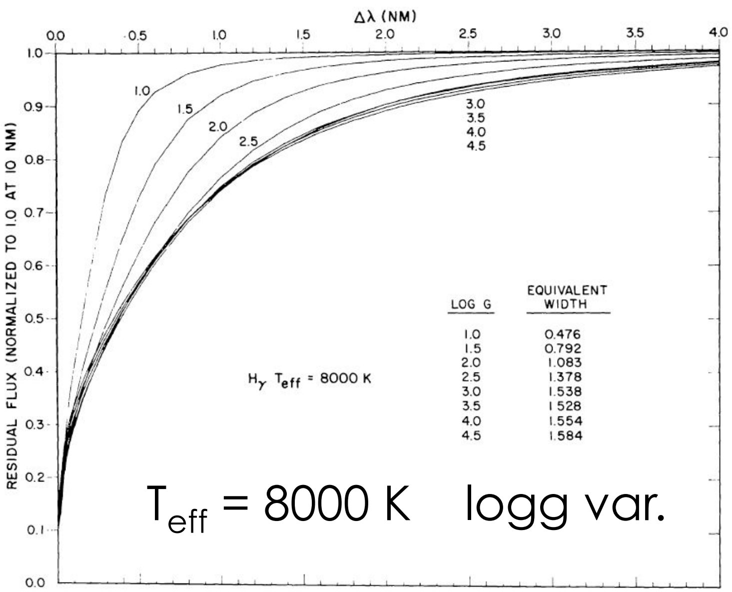

FIG. 24.—Hγ profiles as a function of gravity for T_{eff} = 8000 K

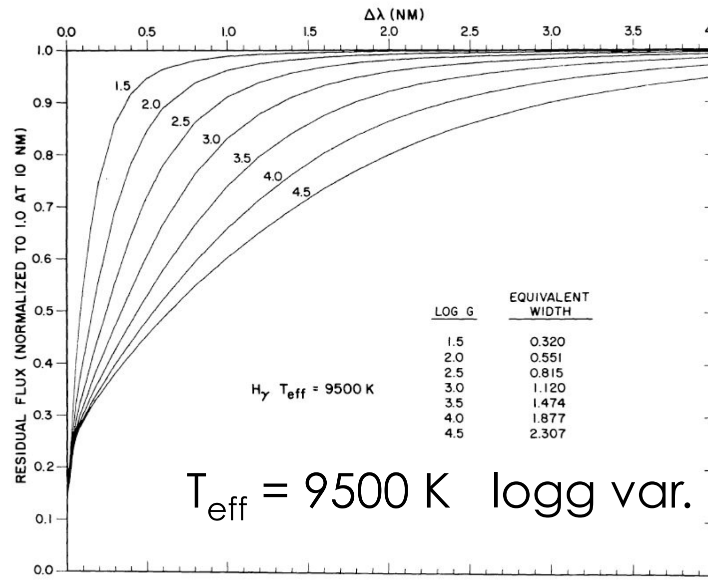

—Hγ profiles as a function of gravity for T_{eff} = 9500 K, roughly A0, where the profile is ideal for gravity determination

T_{eff} determination: Balmer lines vs. photometric calibrations

Sun

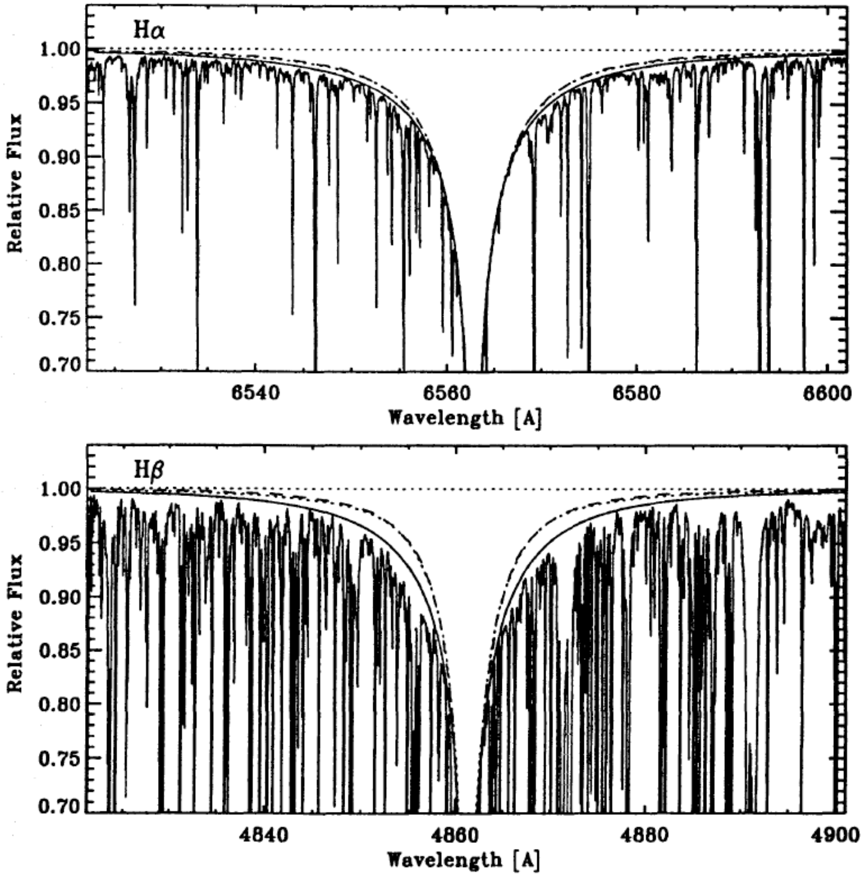

Fig. 2. Solar Hα (top) and Hβ (bottom) line profiles compared with synthetic fit profiles from 3 different solar model atmospheres, Holweger & Müller (1974, dots), Kurucz (1979, $\alpha = 2$, dashes), and our own ODF model ($\alpha = 0.5$, continuous line)

Fuhrmann et al. 1994, A&A, 285, 585

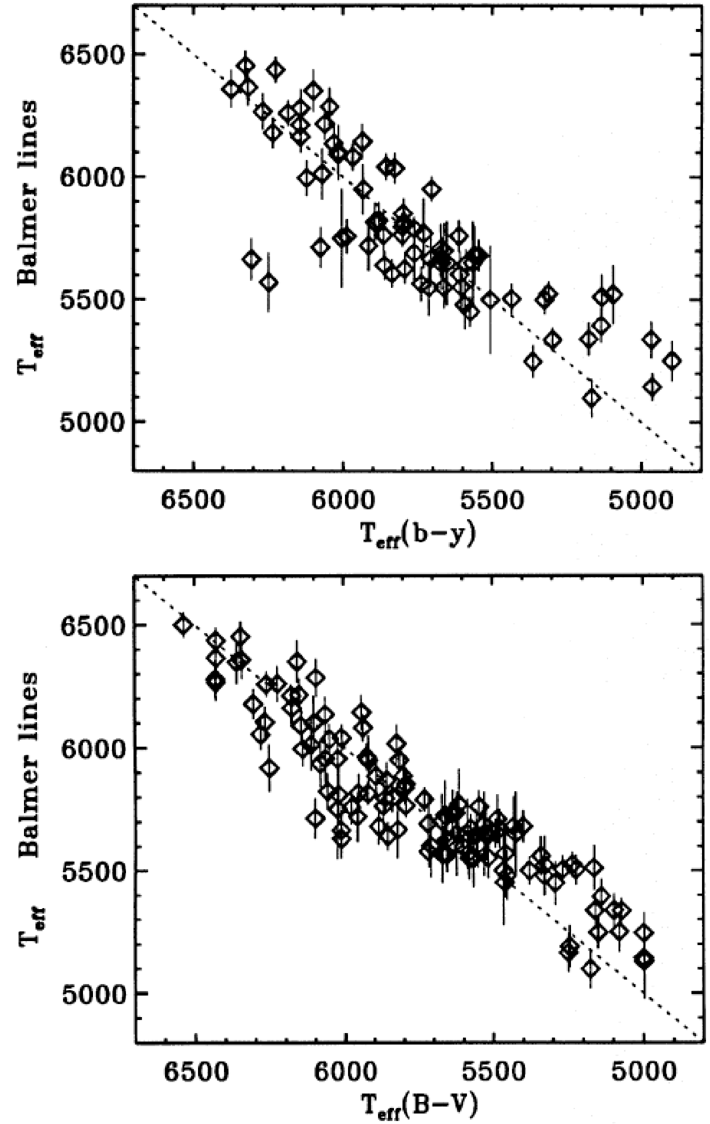

Fig. 4. Effective temperatures obtained from Balmer line fits are compared with colour temperatures derived from b − y (top) and B − V (bottom). The calibration of Magain (1987) is used here (see text)

log *g* determination: LTE Fe I/II ionization equilibrium

Fuhrmann et al. 1997, A&A, 323, 909

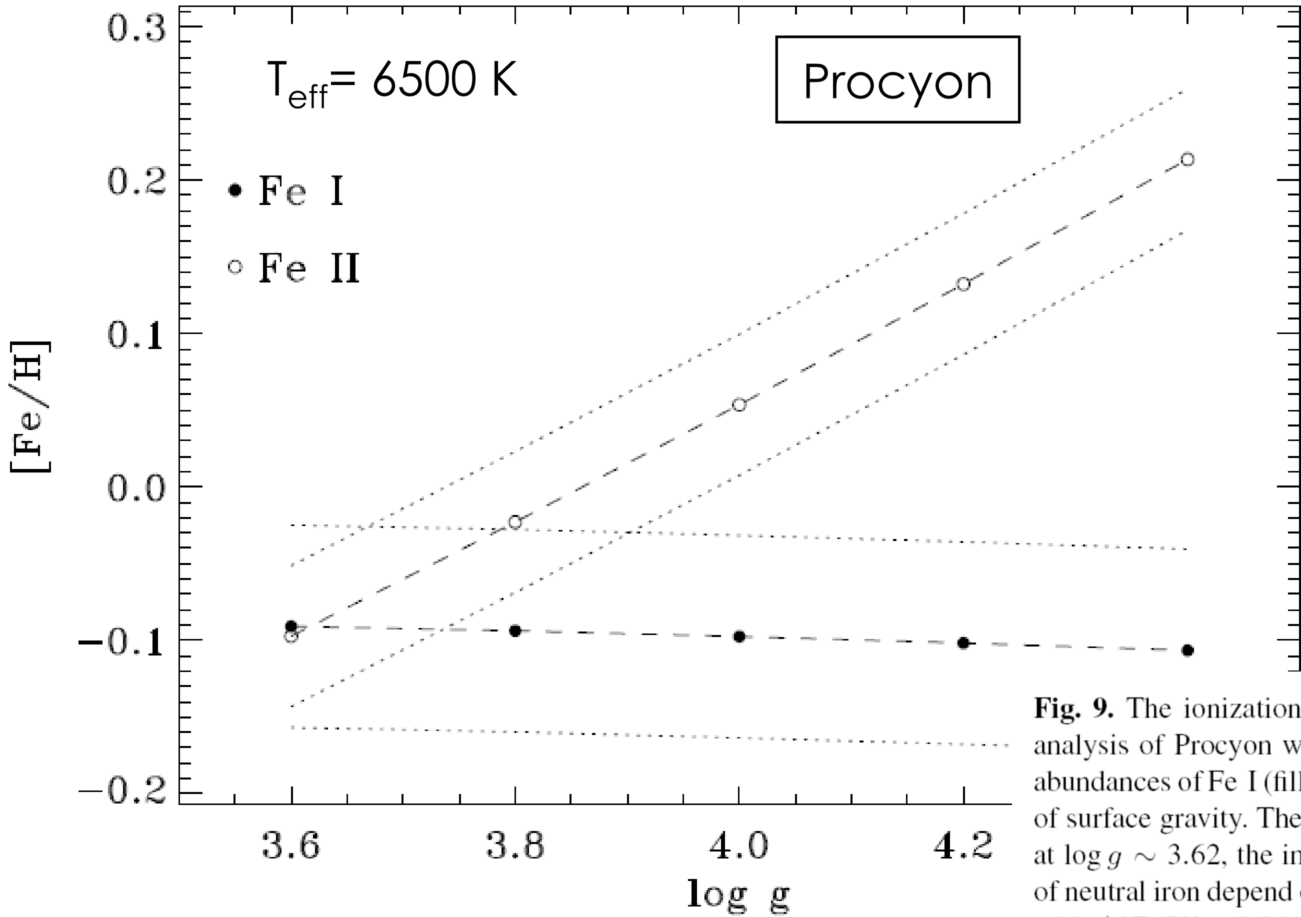

log g $^{FeI/II}$ = 3.58 dex

direct method

log g $^{astrom.}$ = 4.05 dex

Fig. 9. The ionization equilibrium of iron in the model atmosphere analysis of Procyon with T_{eff} = 6500 K. Dashed lines indicate the abundances of Fe I (filled circles) and Fe II (open circles) as a function of surface gravity. The dotted curves are the 1σ error bars (rms) valid at $\log g \sim 3.62$, the intersection of Fe I and Fe II abundances. Lines of neutral iron depend on the precise value of the effective temperature with Δ[Fe/H]∼ 0.06 dex for a change of ΔT_{eff} = 100 K. Fe II instead is very sensitive to the surface gravity parameter, but almost independent to a change in the effective temperature (Δ[Fe/H]< 0.01 dex for ΔT_{eff} = 200 K). The discrepancy at $\log g$ = 4.05, the astrometric surface gravity of Procyon, amounts Δ[Fe/H]= 0.17 dex. To reconcile the Fe I and Fe II abundances an unrealistic high effective temperature of ∼ 6800 K would be required

ionization equilibrium:
same abundance from all ions
at one set of parameters

log *g* determination: Mg line wings

Fuhrmann et al. 1997, A&A, 323, 909

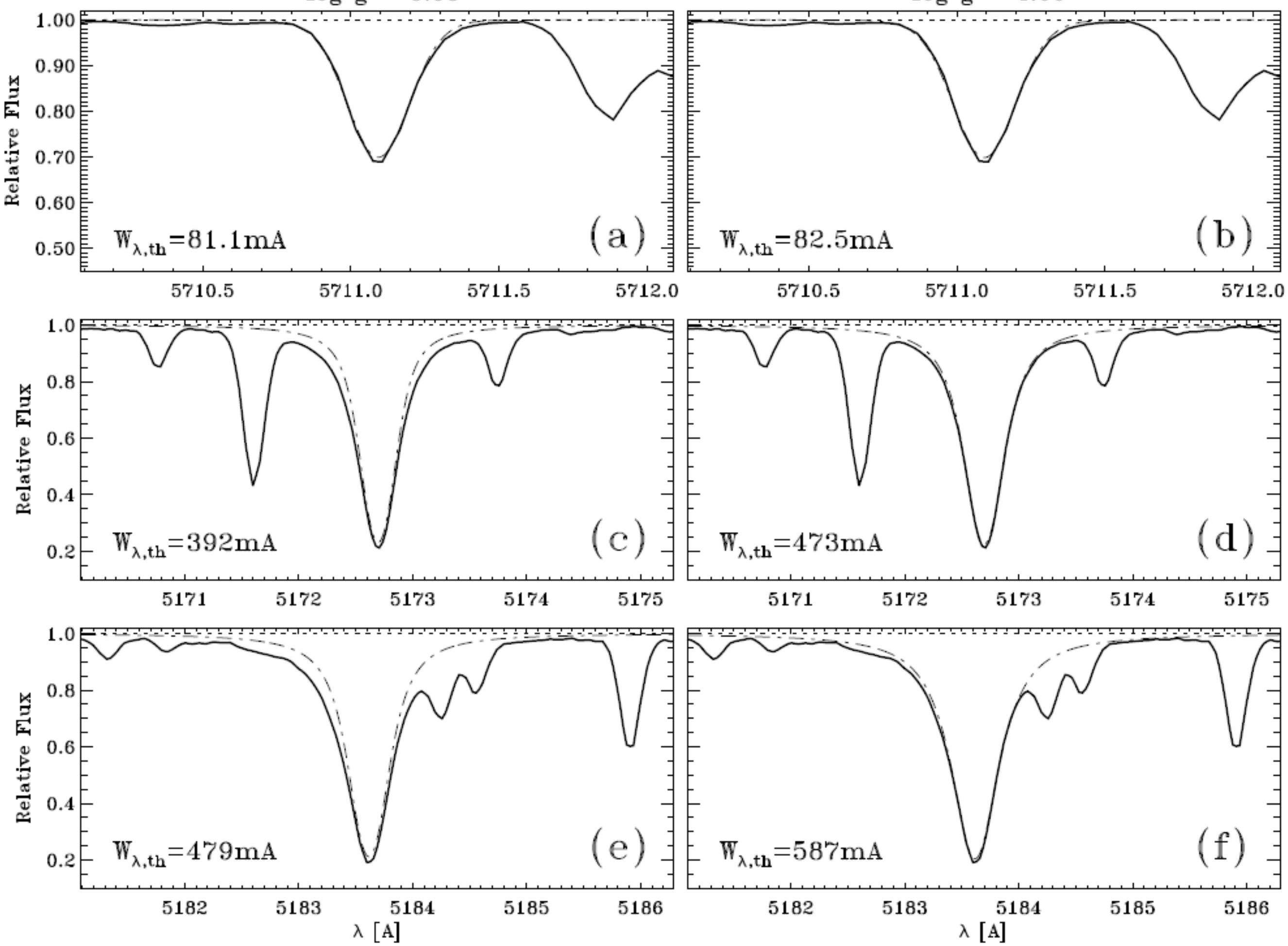

T_{eff}= 6500 K

log g ^{Mg} = 4.00 dex

direct method

log g $^{astrom.}$ = 4.05 dex

consistency in LTE

Fig. 10a–f. The spectroscopic surface gravity determination of Procyon from the analysis of Mg I lines. Left column: line profiles of Mg I λ5711 (top) and the Mg Ib lines λ5172 and λ5183 (below) for a surface gravity value log g = 3.58, as derived from the ionization equilibrium. The profile of λ5711 shows no wings and is practically independent of the surface gravity, as illustrated in panel **b** , where line formation is done for a value log g = 4.00. Among other weak Mg I lines, λ5711 therefore serves to fix the value of the Mg I abundance. This information is *then* used in the analysis of λ5172 and λ5183 by altering the surface gravity value until the observed line shape is reproduced as shown in panels **d** and **f** . In the case of Procyon log g = 4.00 is found by this method, which is 0.42 dex higher than derived from the ionization equilibrium and only slightly below log g = 4.05, the very precisely known value from astrometric data

NLTE Refinements

Status of Hα modelling in the Sun: LTE ...

Cowley & Castelli 2002, A&A, 387, 595

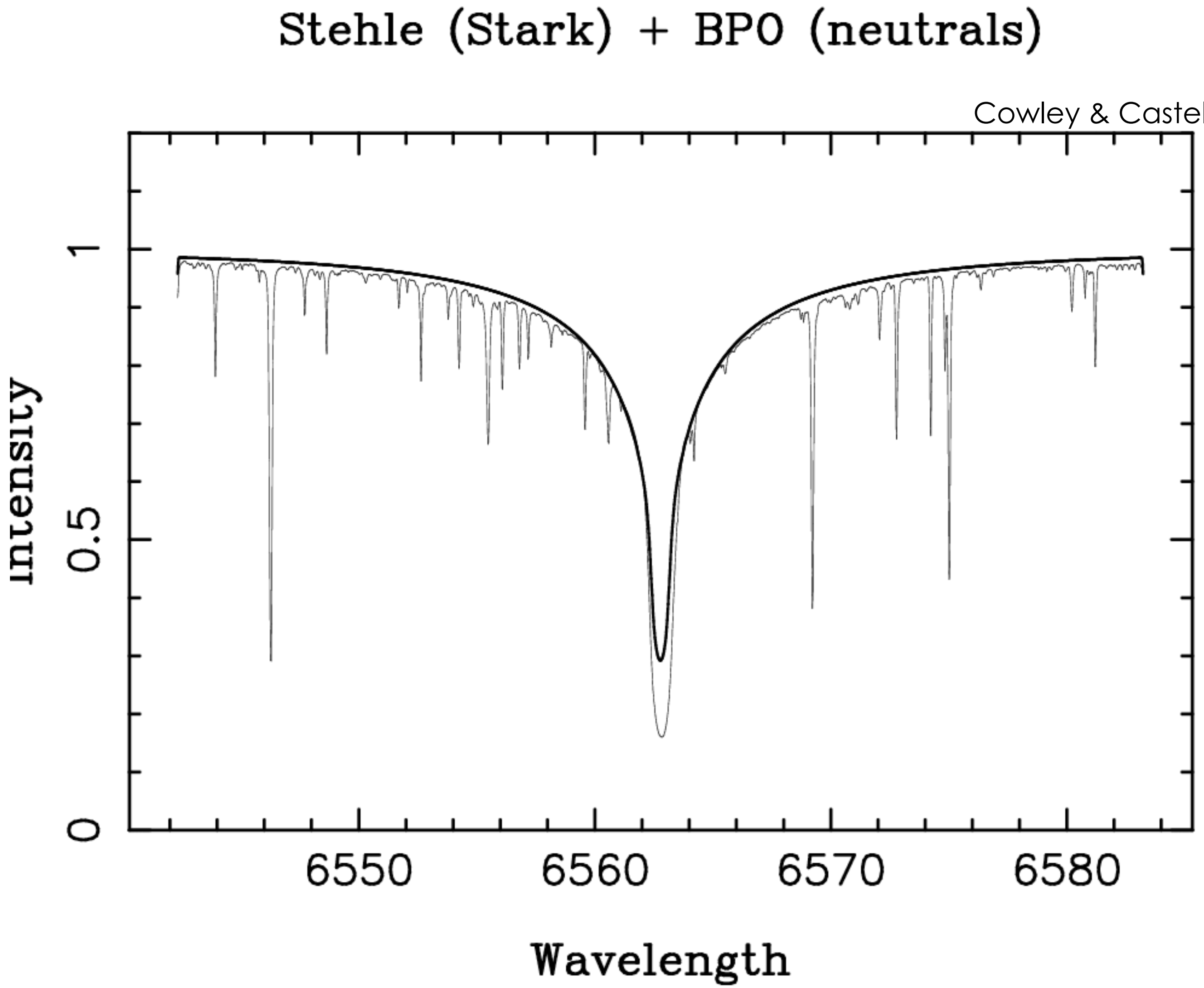

... and NLTE

Przybilla & Butler 2004, ApJ, 610, L61

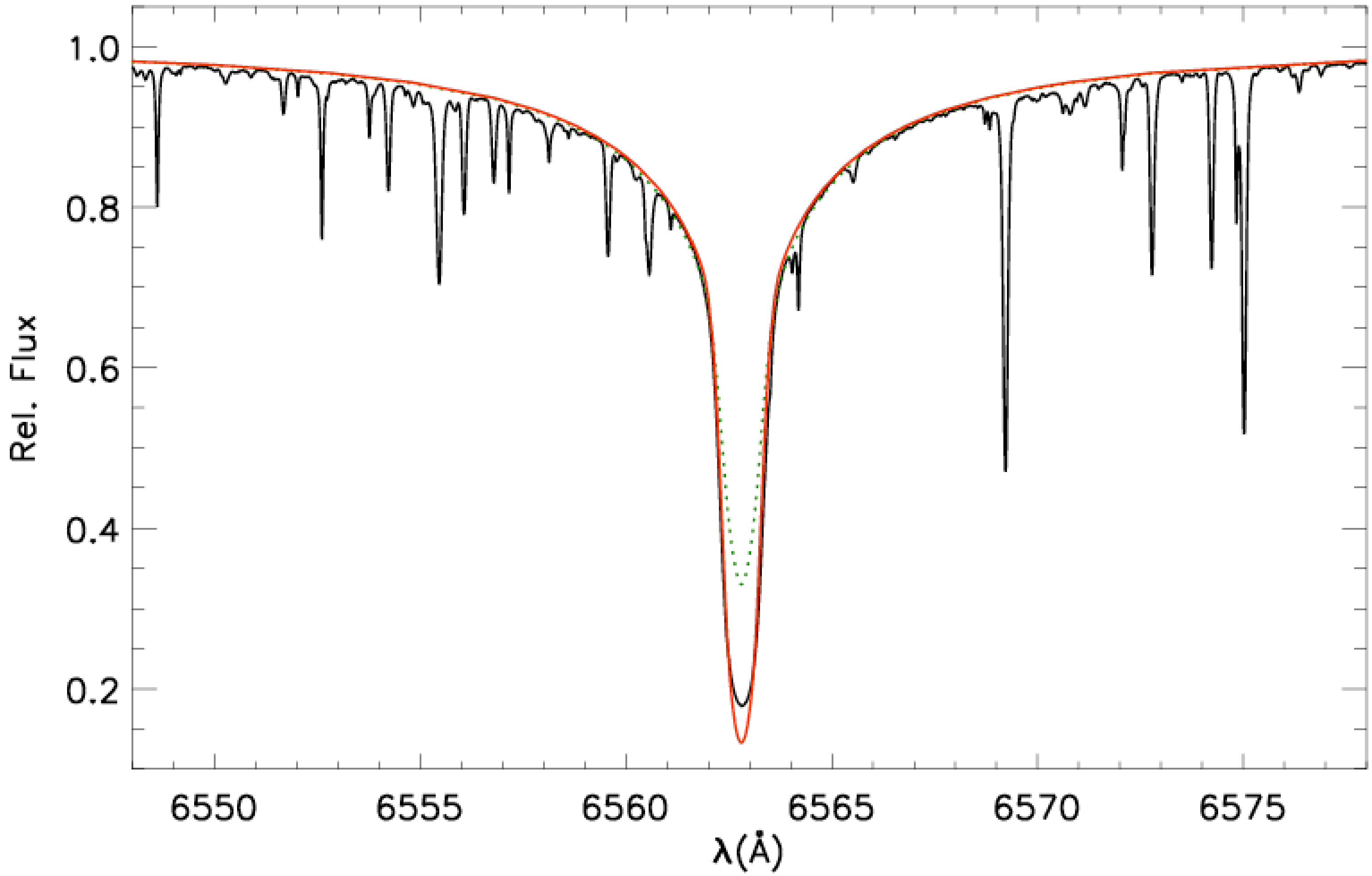

- chromosphere important:
  line-formation depth as observational discriminator

Sun: the broader picture in NLTE

Przybilla & Butler 2004, ApJ, 610, L61

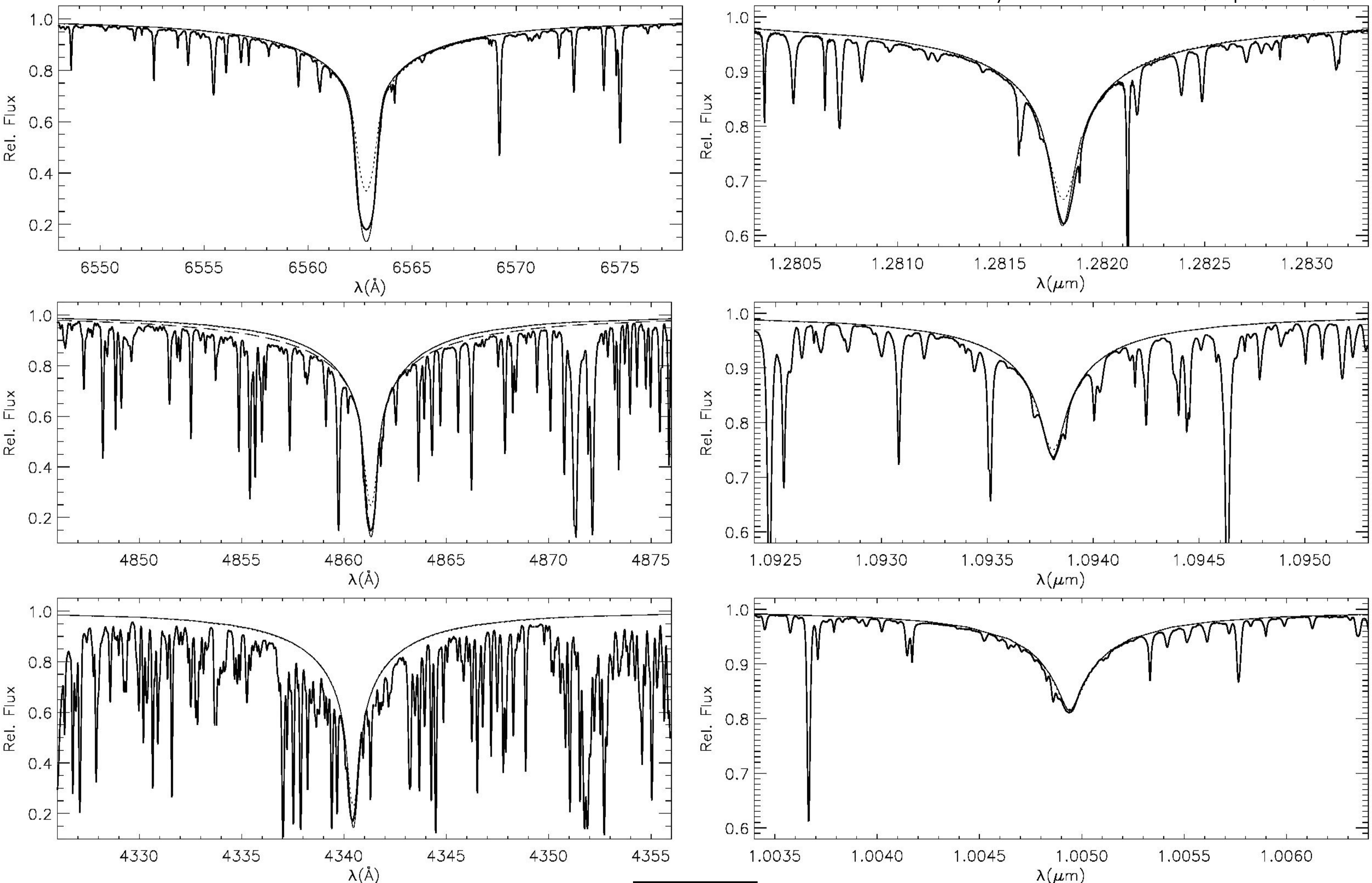

$S_H=2$

Arcturus: metal-poor K giant

Przybilla & Butler 2004, ApJ, 610, L61

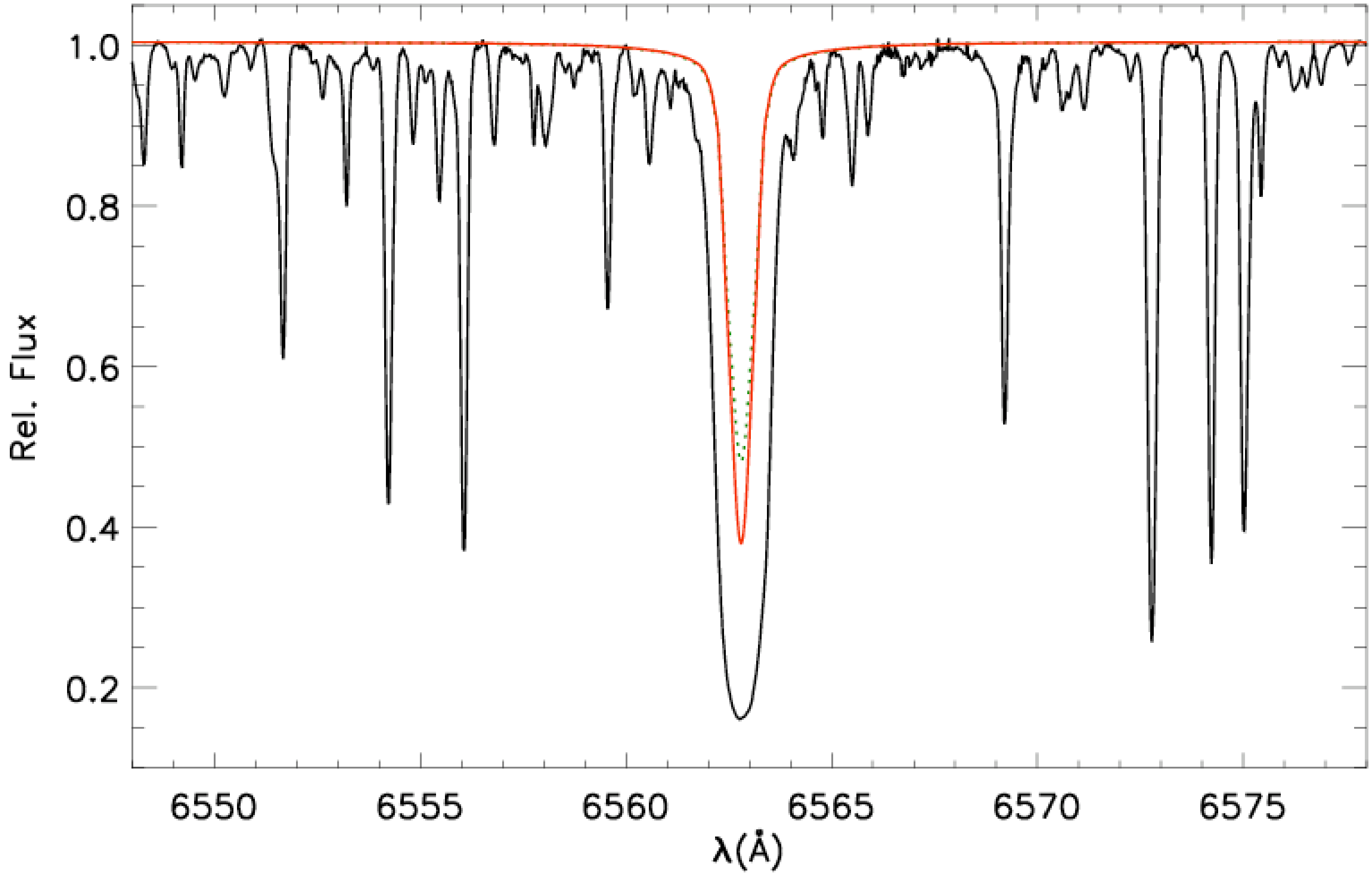

- model atmosphere (Kurucz) used reproduces metal line spectrum

Gummersbach et al. 1998, A&A, 338, 881

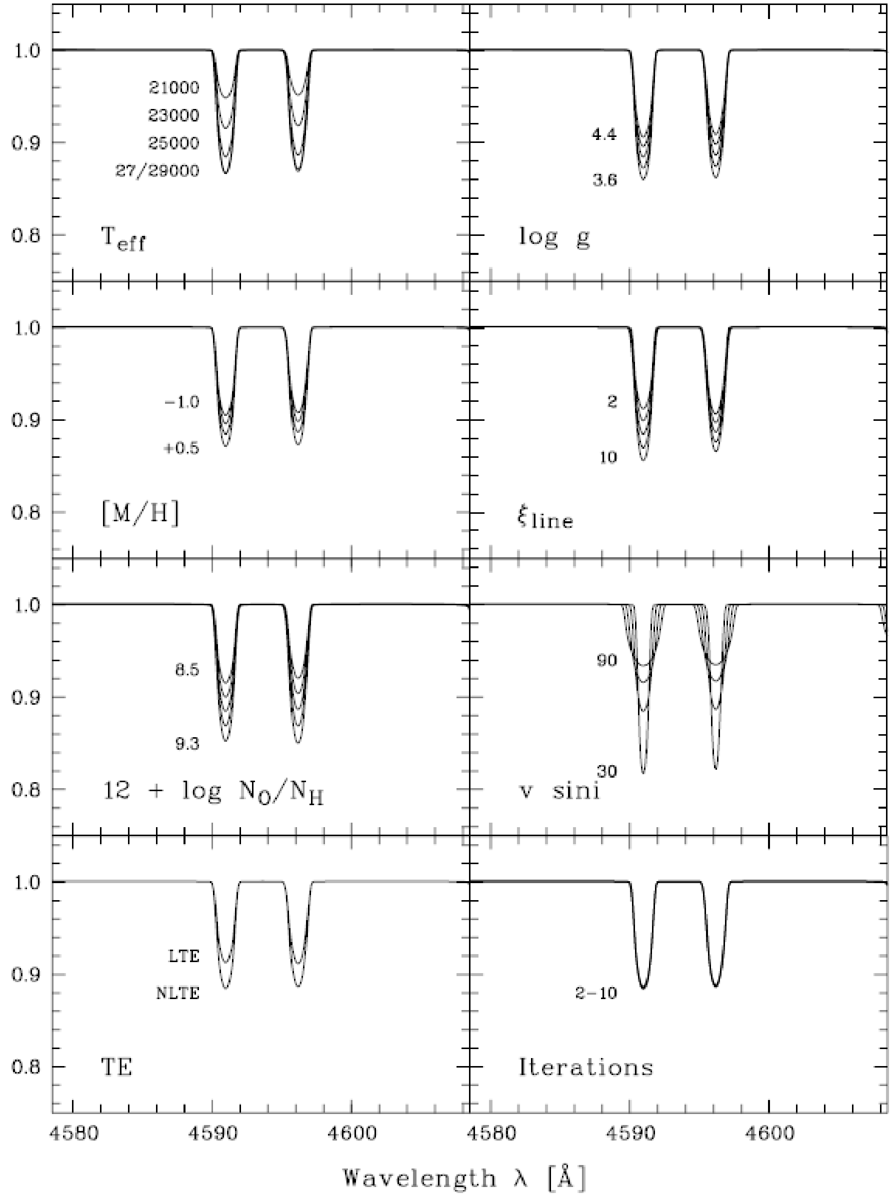

Fig. 4. Same as Fig. 3, for O II 4591/96 and $X_{\mathrm{O}} = 8.9$. Note the different behavior of [M/H].

Effects to consider for stellar parameter/abundance determination

NLTE one among many factors

➡ all need to be met

T_{eff}= 25000 K, log g= 4.0

using Becker & Butler model atoms

Gummersbach et al. 1998, A&A, 338, 881

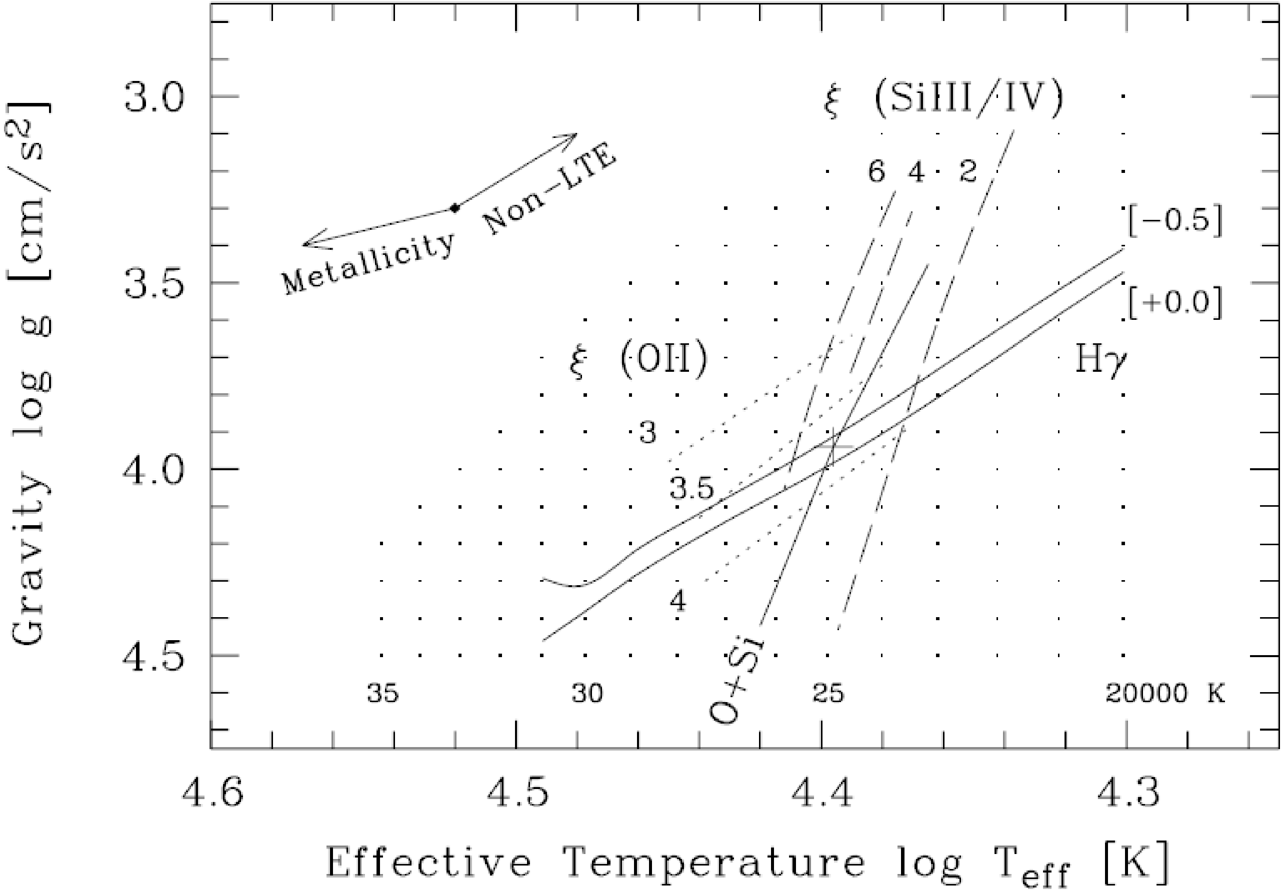

Fig. 8. Overall analysis: Hydrogen analysis as function of [M/H]=0 and -0.5 (*solid*), silicon analysis as function of ξ (*dashed*), oxygen analysis as function of ξ (*dotted*), combined silicon and oxygen analysis (*solid*), and the derived stellar parameters (+) for SH 2-208/6. The arrows denote the metallicity effect of sub-solar atmospheres and the non-LTE effect discussed in Sect. 9.

Kiel diagram

highly useful for diagnostics

T_{eff}= 25000 K, log g= 4.0

using Becker & Butler model atoms

Explicitly...
chemical abundances rely on:

- model atmospheres
- model atoms
- solution SE & RT: numerics
- other input: e.g. background opacities
- quantitative analysis (e.g. atmospheric parameters adopted)
- quality of observed spectra
- ...

All are potential sources of systematic uncertainties

Self-consistent method

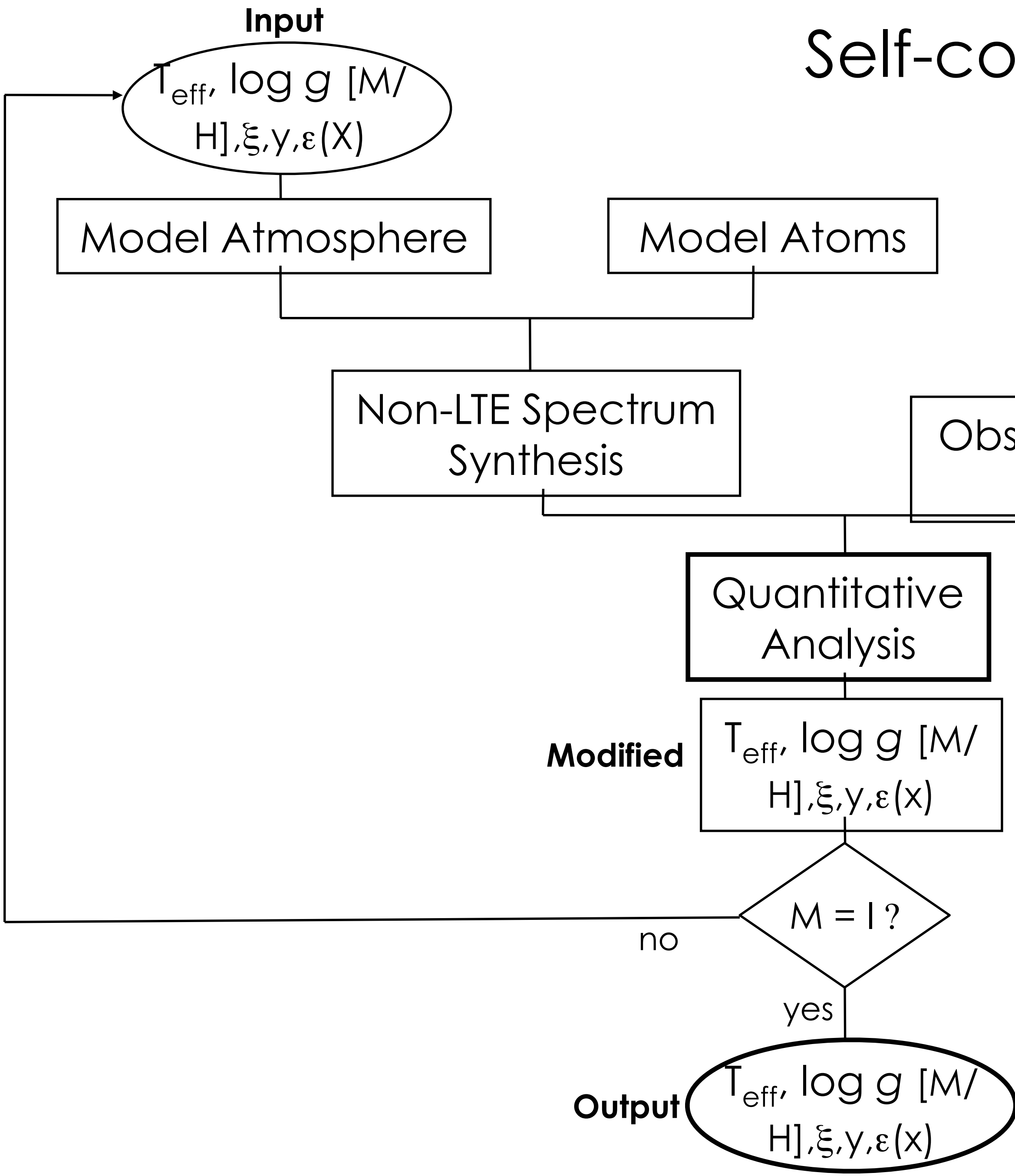

Simultaneous atmospheric parameter & metal abundance derivation

Quantitative analysis

Independent constraints for atmospheric parameters:

- H & He lines
- multiple ionization equilibria
- SEDs

- $\Delta\ T_{eff}\ /\ T_{eff}\ \sim 1\%$
- Δ log g ~ 0.05…0.10 (cgs)

} can be achieved

E.g. parameter determination in :

Early-B type dwarf/giant stars
&
A-type supergiants

- log *g* & T_{eff}: hydrogen lines (Balmer, Paschen, ...)
- log *g* & T_{eff}: ionization equilibria (He, metals)
- ξ: ε(X) from line analysis vs. observed W_λ
- y: He lines
- [M/H]: abundance analysis
- v sin i & ζ: line analysis
- additional constraints: SED's, near-IR ...

T_{eff} and log *g* effects on hydrogen lines

E.g. A supergiant

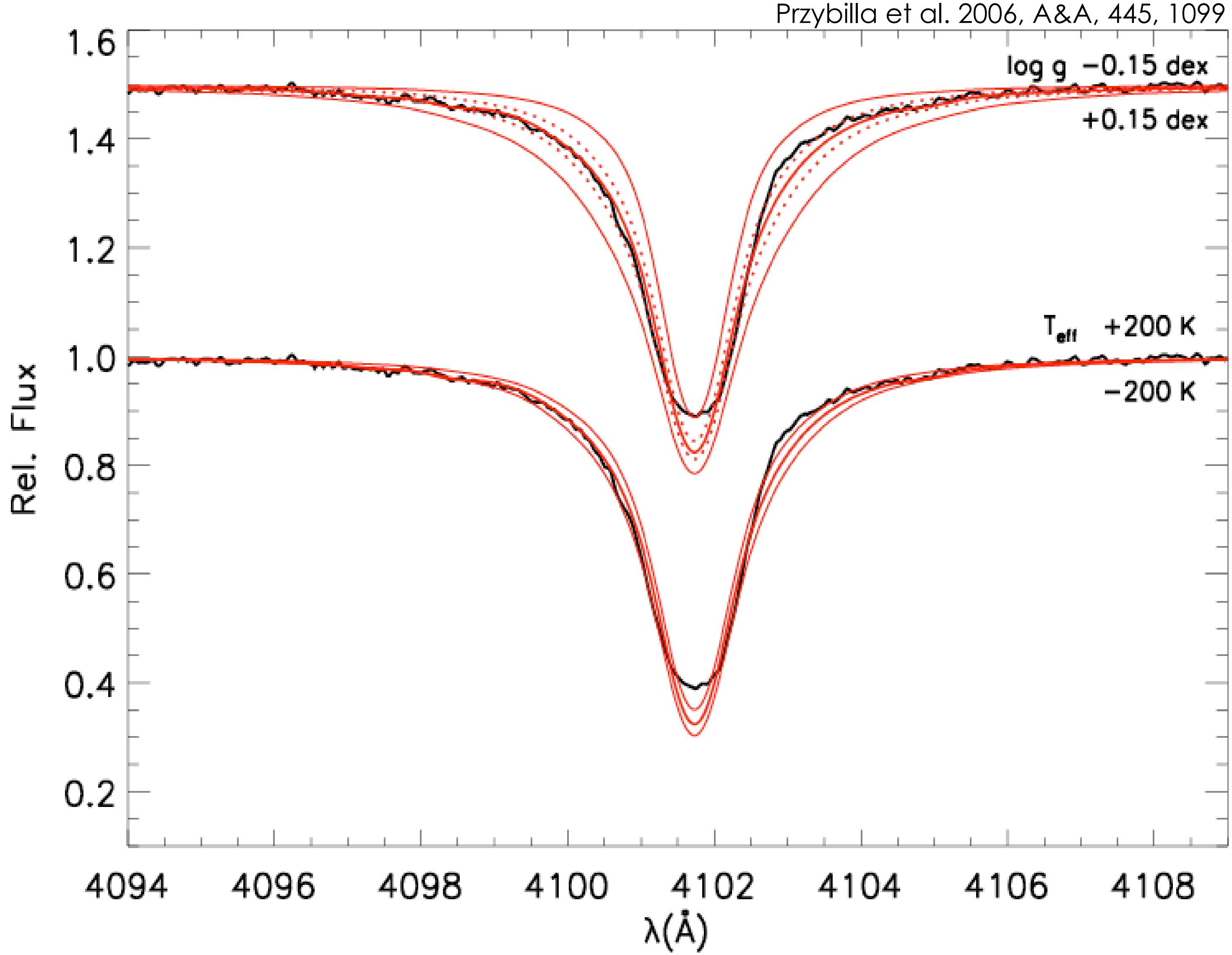

T_{eff} and log *g* effects on metal lines

E.g. A supergiant

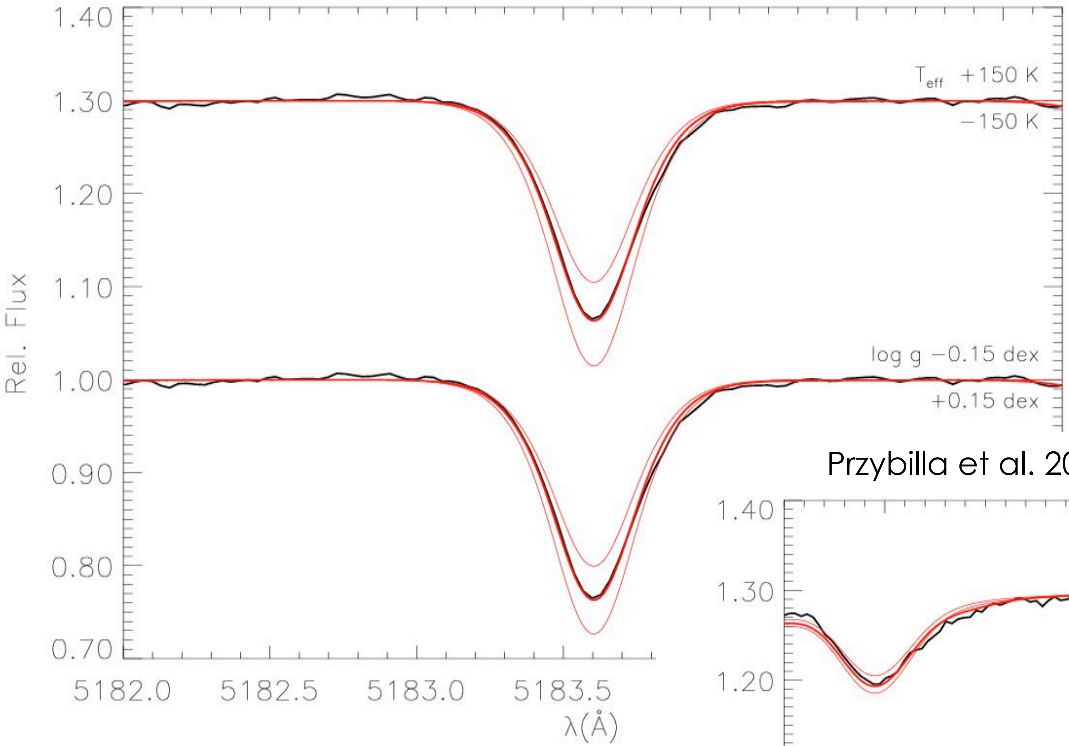

Mg I sensitive

Przybilla et al. 2006, A&A, 445, 1099

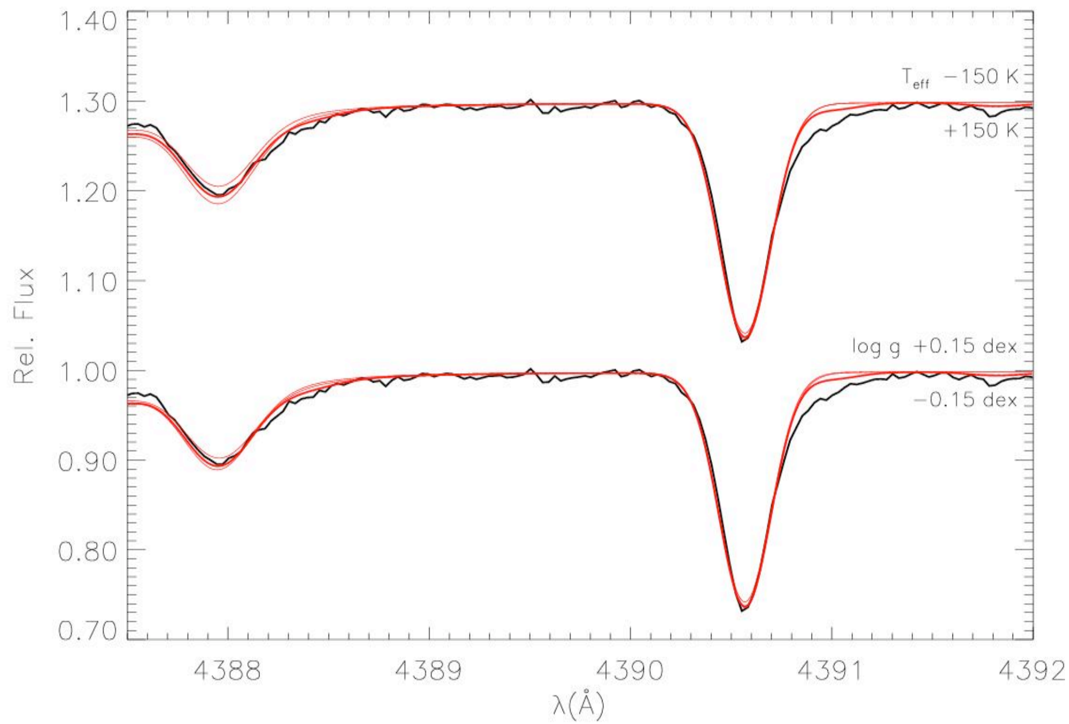

Mg II non-sensitive

→ ionization equilibrium

T_{eff} & log *g* determination from independent indicators

Przybilla et al. 2006, A&A, 445, 1099

E.g. A supergiant

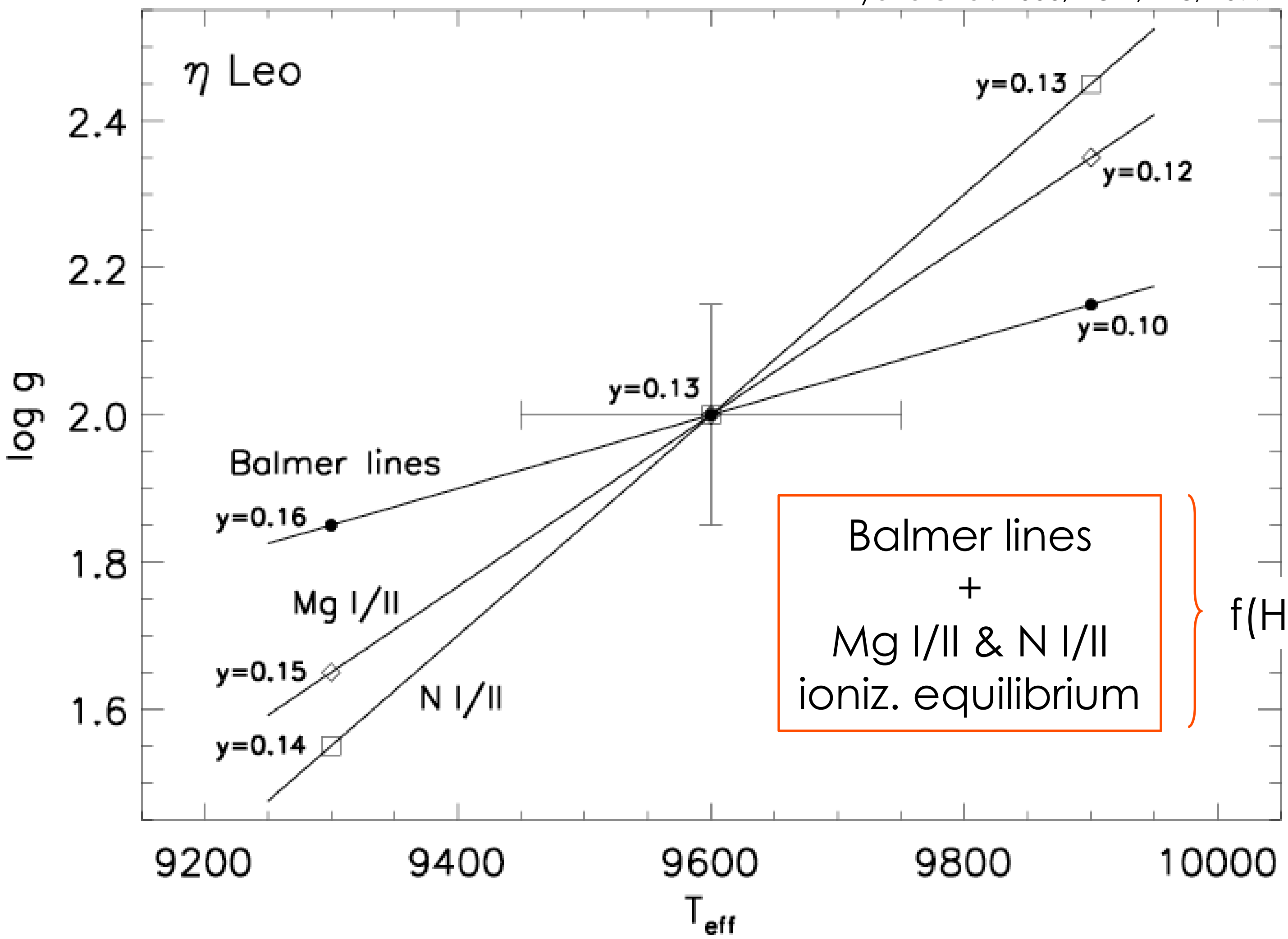

Balmer lines
+
Mg I/II & N I/II
ioniz. equilibrium

} f(He abund.)

Reduced uncertainties

Additional constraint: SEDs

E.g. A supergiant

Przybilla et al. 2006, A&A, 445, 1099

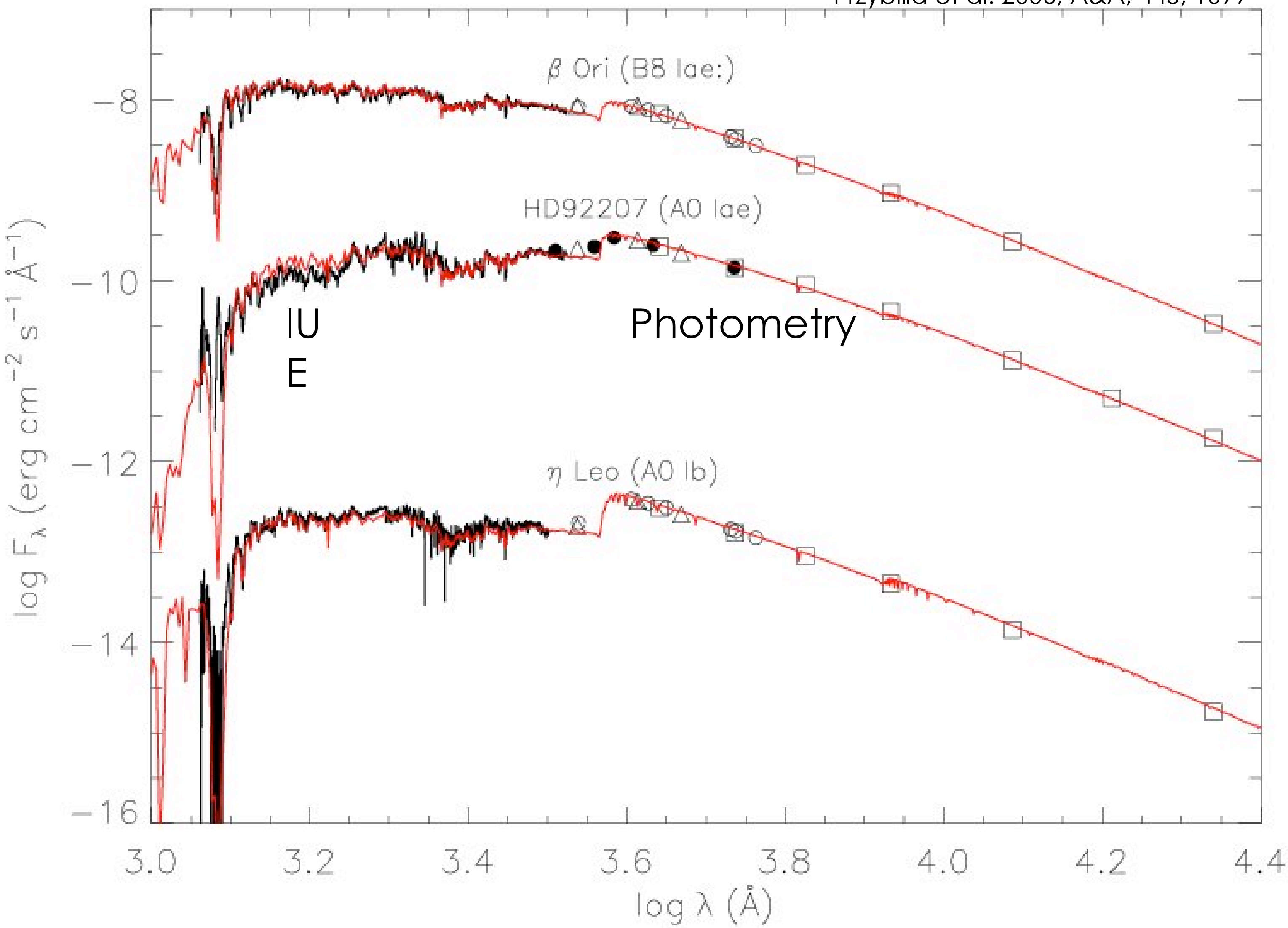

Macroturbulence & *v* sin *i* from metal line profiles

Przybilla et al. 2006, A&A, 445, 1099

E.g. A supergiant

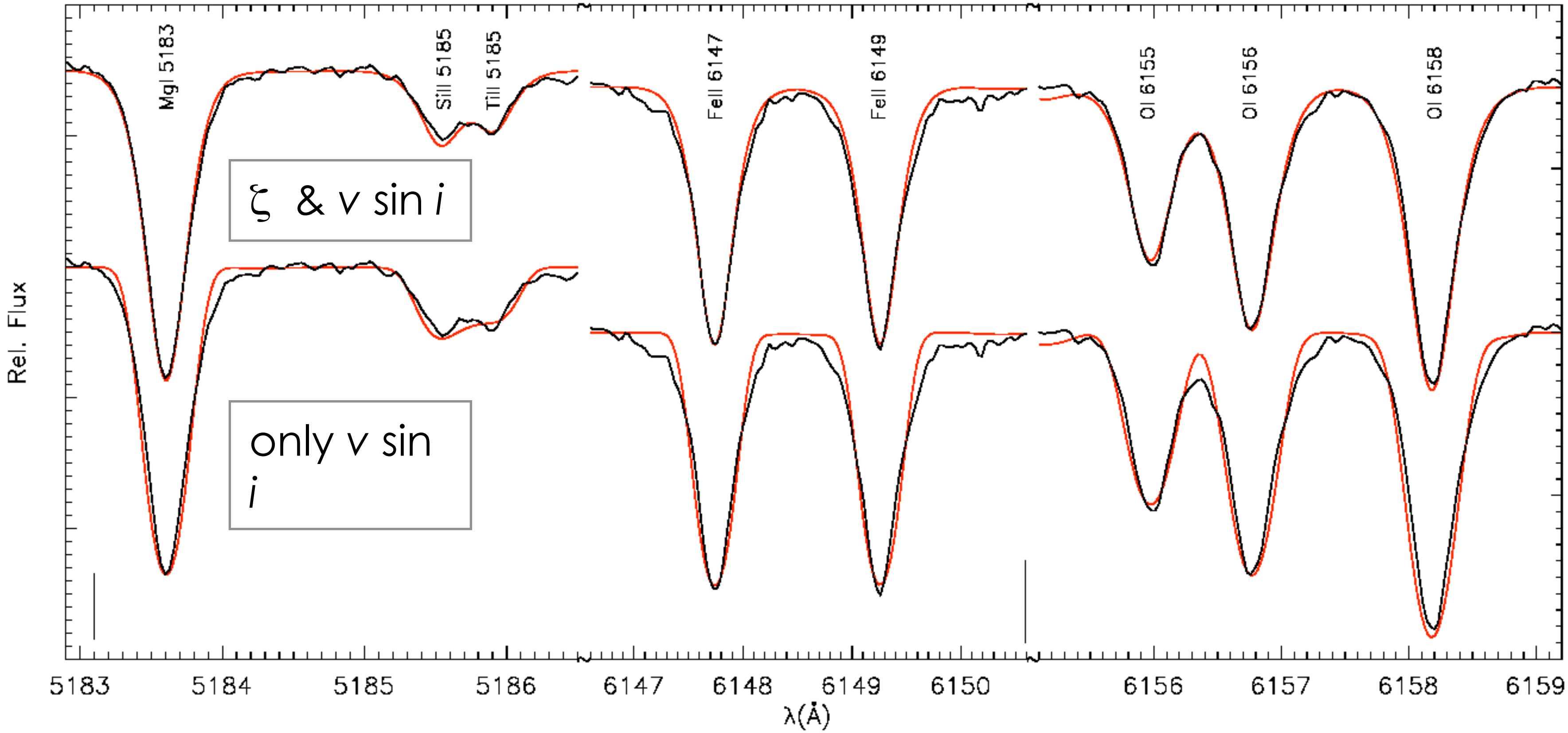

Advantage of line profiles over equivalent widths

Microturbulence effects on ionization equilibria

E.g. early B dwarf

Nieva, 2007, Ph.D. thesis

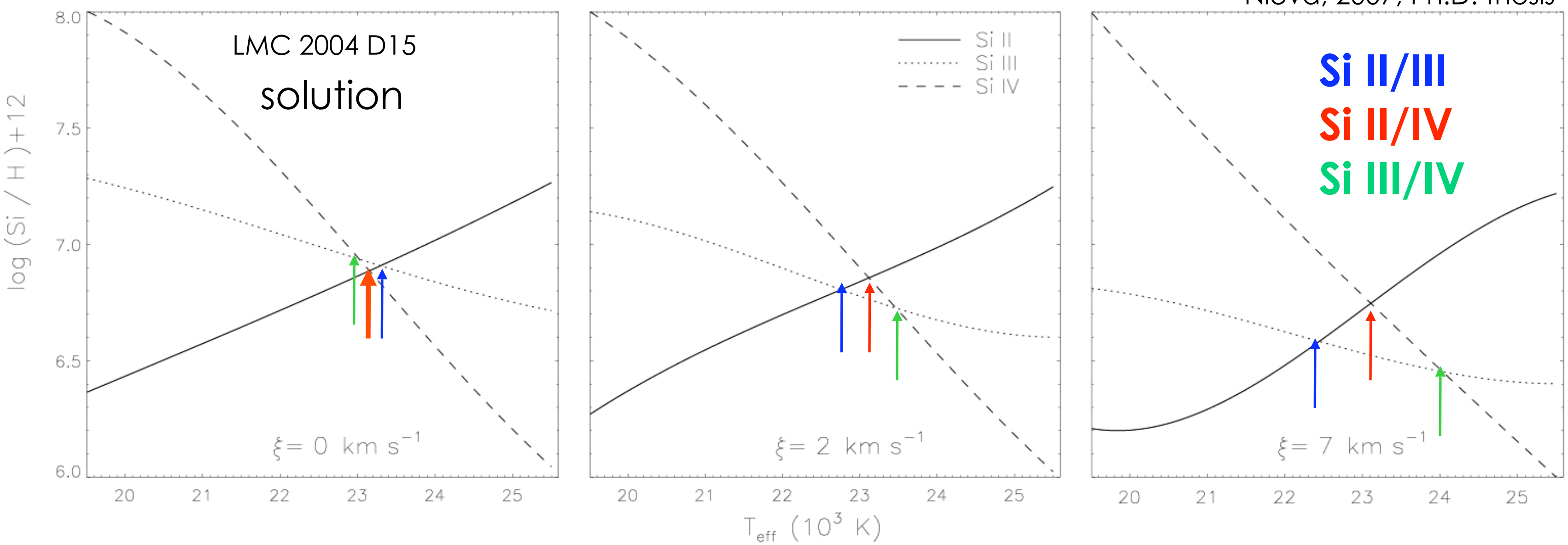

@ ~23000 K **Si II/IV** lines weak & **Si III** lines strong: sensitive to ξ

Implicit fit to Balmer lines for each T_{eff} (log *g* determination)

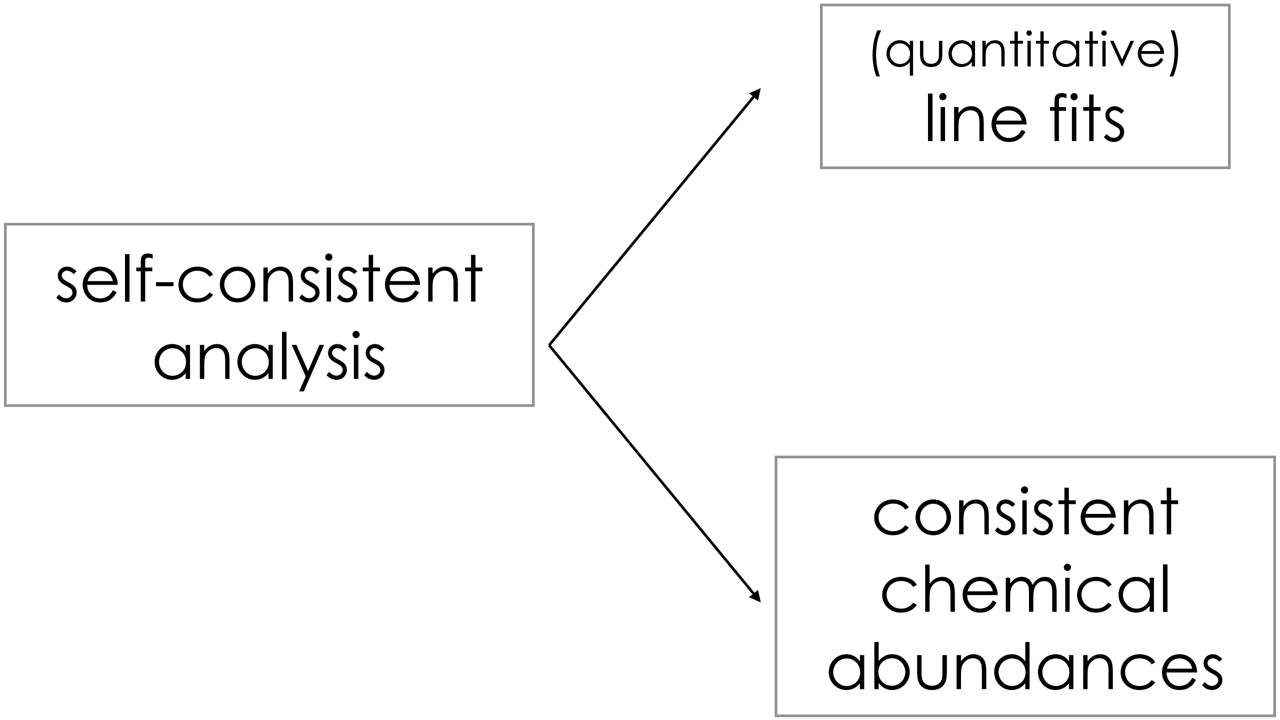
self-consistent analysis
(quantitative) line fits
consistent chemical abundances

Simultaneous fits to most measurable H/He lines

Visual

Nieva & Przybilla 2007, A&A, 467, 295

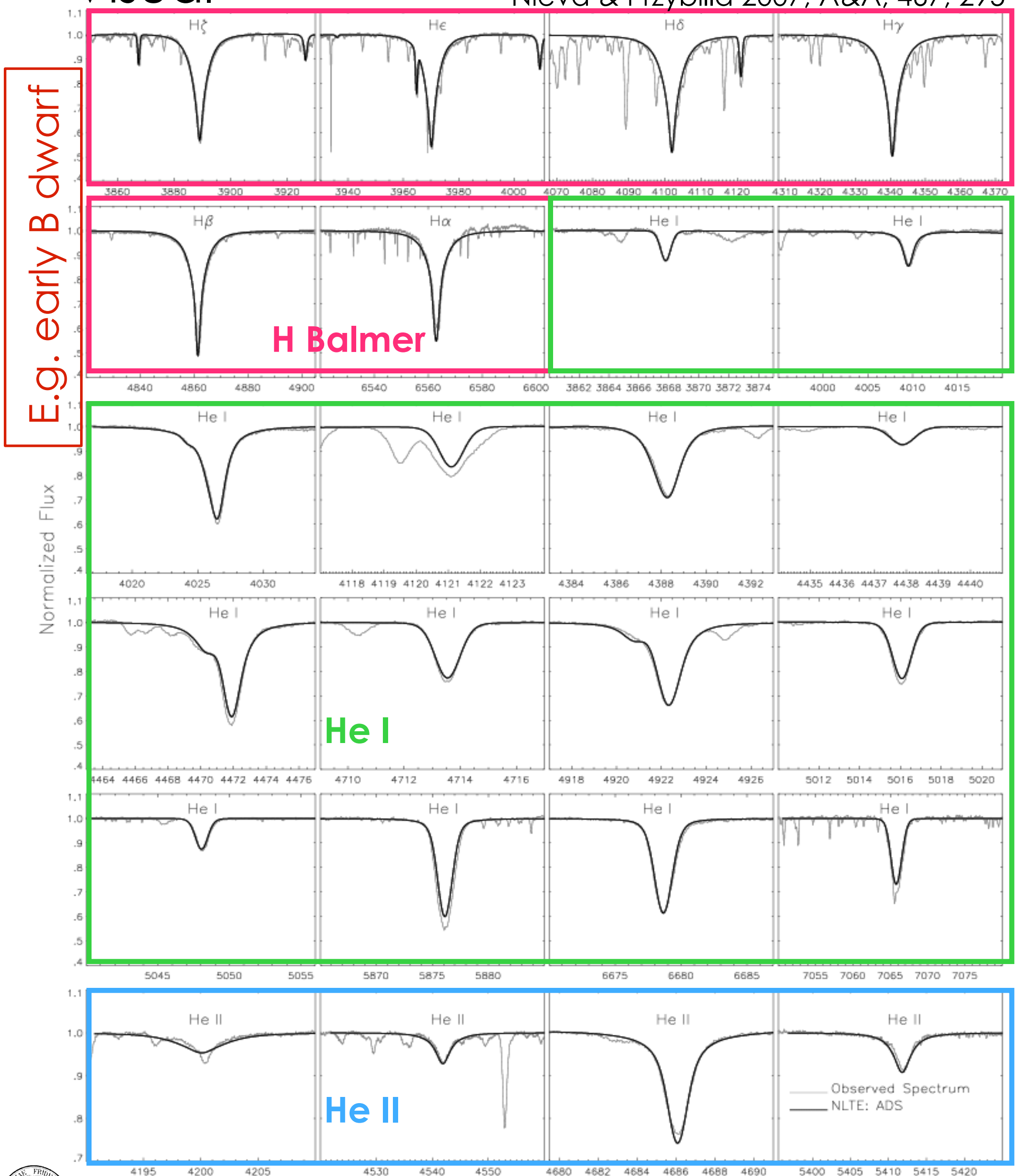

Near-IR

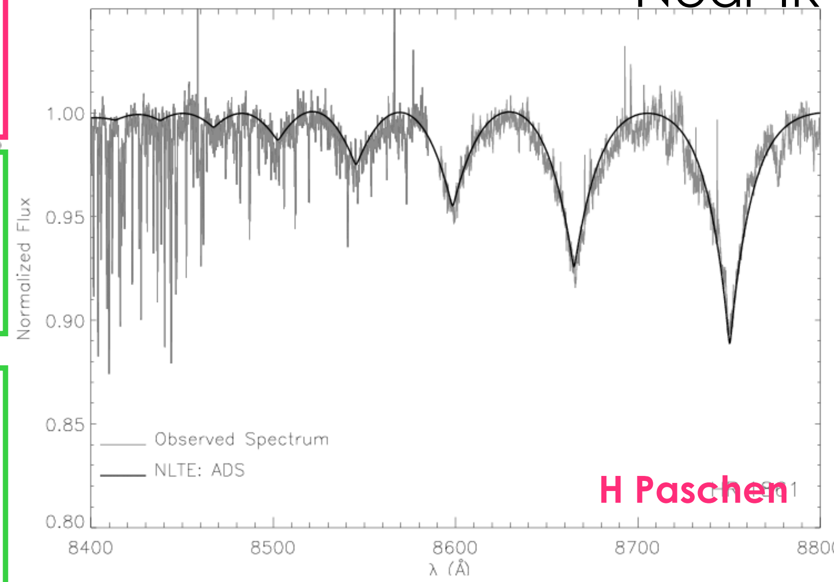

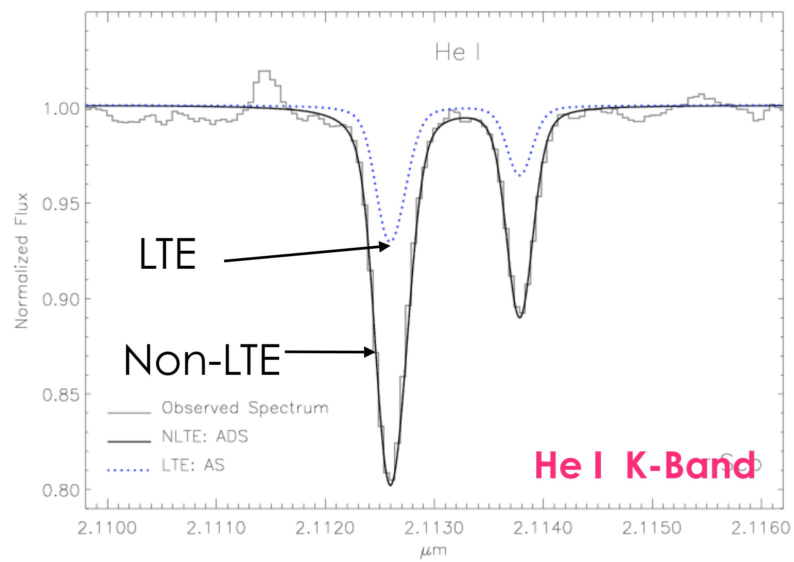

Fits to C lines

E.g. early B dwarf

All lines have very similar abundances

(low 1σ-uncertainties)

Nieva & Przybilla 2007, A&A, subm.

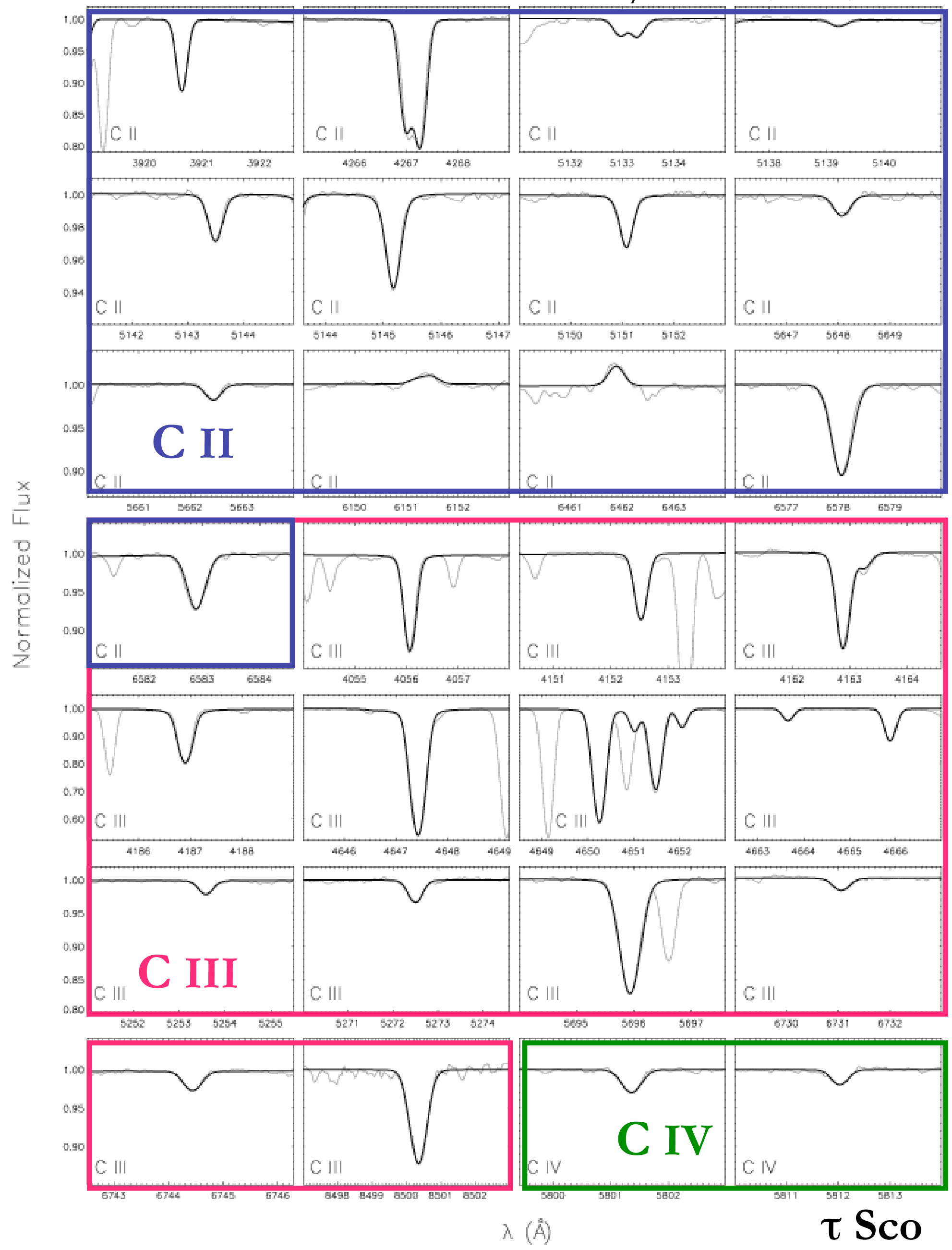

Systematic Uncertainties

E.g. atmospheric structure & stellar flux

Nieva & Przybilla 2007, A&A, 467, 295

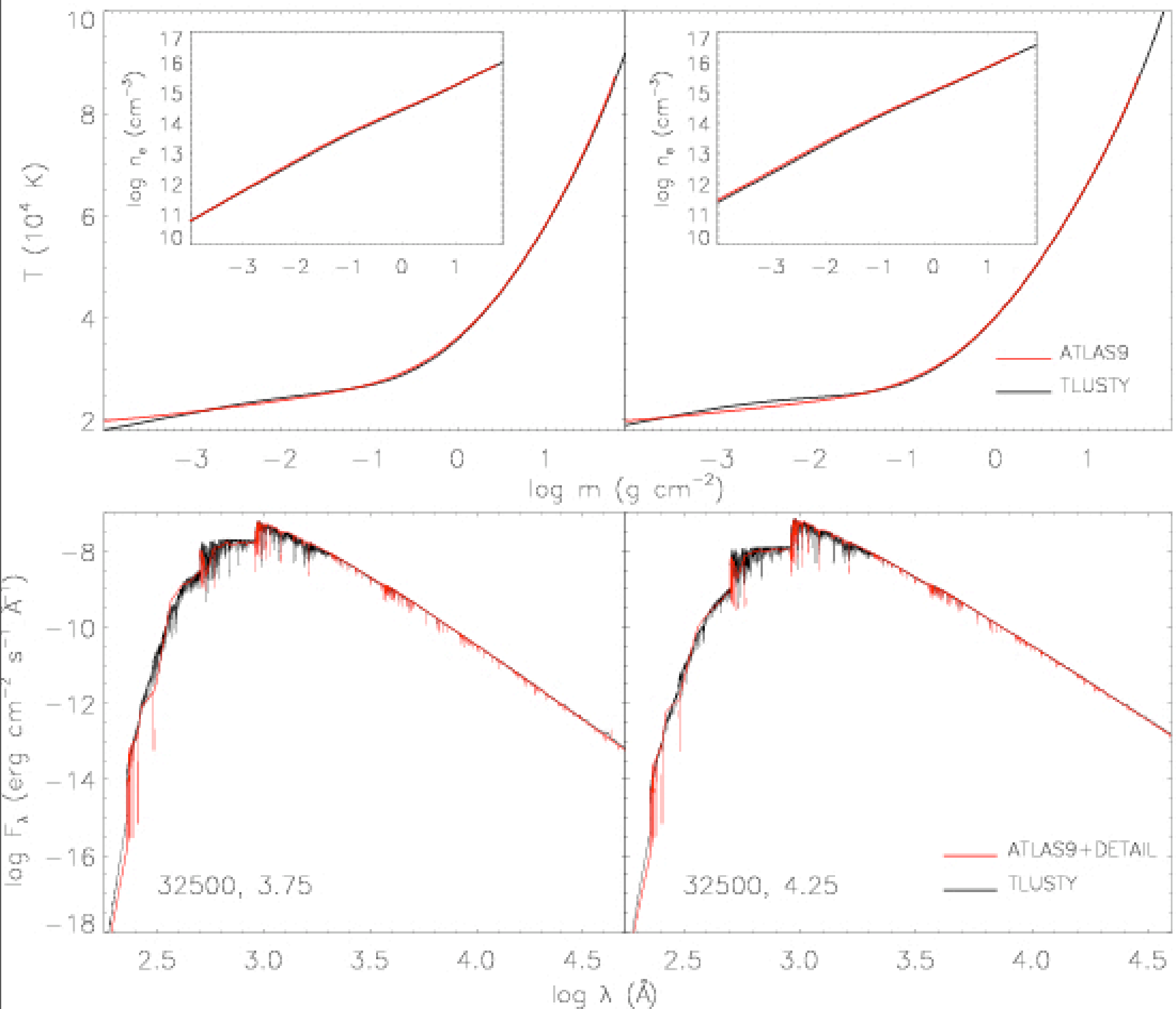

metallicity correction: up to ~500 K in line-formation region

Also:

microturbulence
background
opacities ...

E.g. sensitivity of C II/III/IV abundances to T_{eff}, log g & ξ variations

Nieva & Przybilla 2007, A&A, subm.

E.g. early B giant

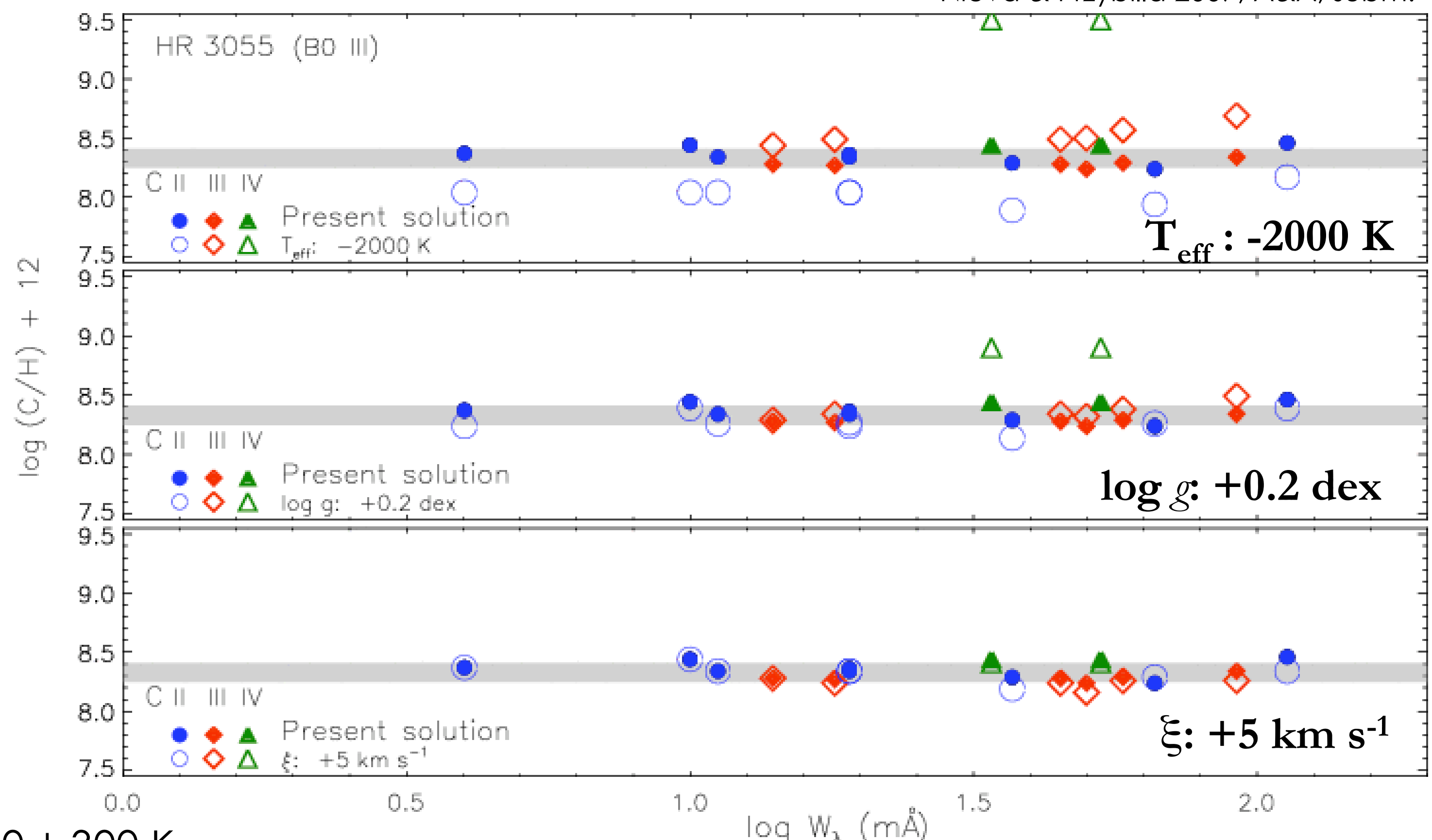

HR 3055

Solution:

T_{eff} = 31200 ± 300 K

log *g* = 3.95 ± 0.05 dex

ξ= 8 ± 1 km s^{-1}

Main effect from T_{eff}

C IV up to +1.10 dex (~x10)
C III up to +0.35 dex (~x2.5)
C II up to -0.40 dex (~x2.5)

T_{eff} vs. NLTE effects on C abundances

(relative to final results)

E.g. early B giant

HR 3055

Present solution:
T_{eff} = 31200 ± 300 K
log g = 3.95 ± 0.05 dex
ξ = 8 ± 1 km s^{-1}

		ΔT_{eff}=-2000 K	LTE
C II	4267	**-0.33**	**-0.40**
	5145	**-0.32**	**0.00**
	5662	**-0.33**	**0.00**
	6578	**-0.40**	**0.00**
C III	4056	**+0.21**	**+0.08**
	4162	**+0.28**	**+0.25**
	4186	**+0.35**	**+0.07**
	4663	**+0.22**	**+0.22**
C IV	5811	**+1.06**	**+0.39**

Nieva & Przybilla 2007, A&A, subm.

NLTE Results

Consistency is possible after careful modelling & analysis

Non-LTE vs. LTE for individual C lines

6 stars

Nieva & Przybilla 2007, A&A, subm.

E.g. early B stars

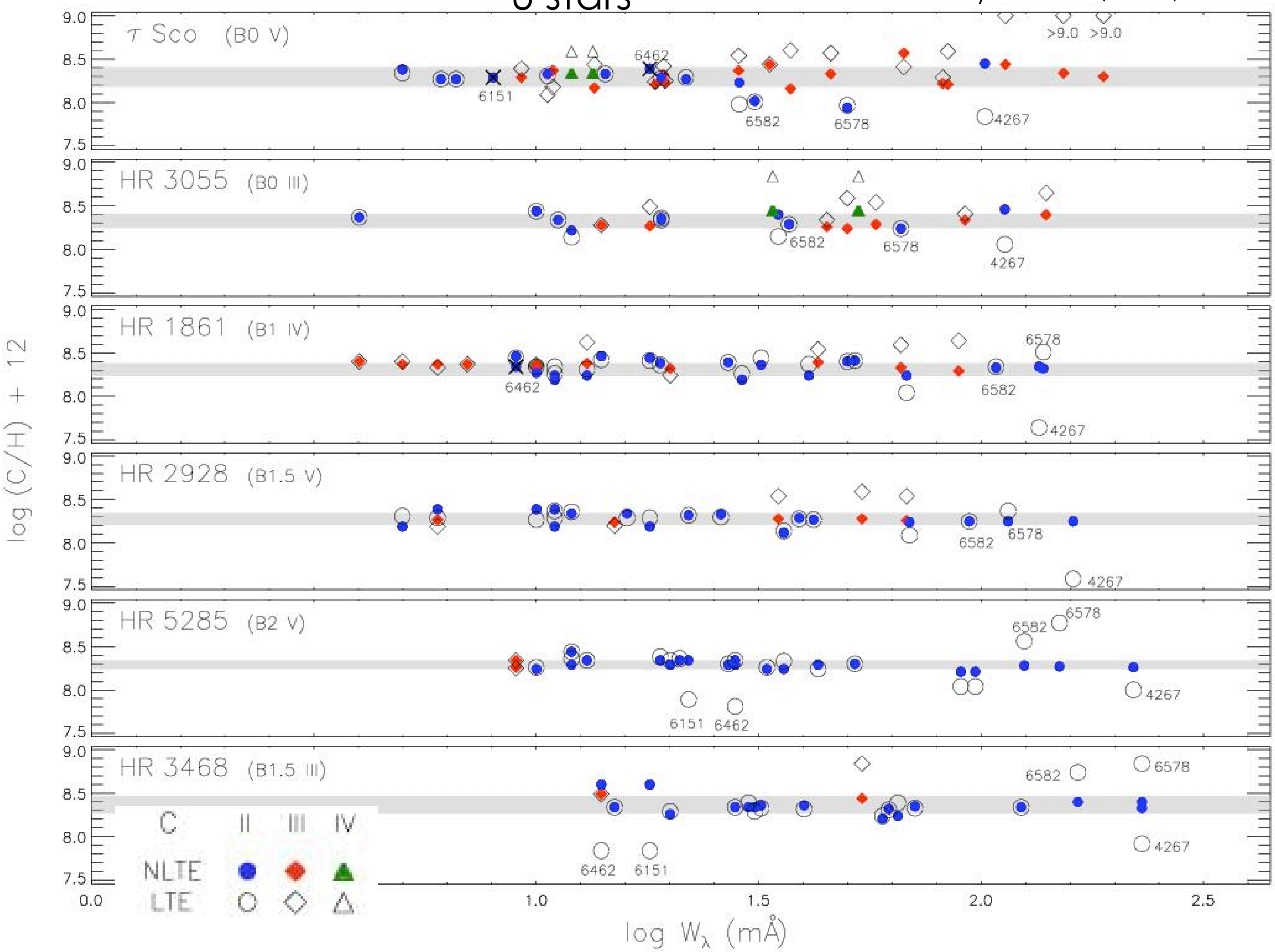

• NLTE effects different per line & star: constant correction not applicable

Non-LTE vs. LTE chemical abundances

E.g. A supergiant

1 star   Przybilla et al. 2006, A&A, 445, 1099

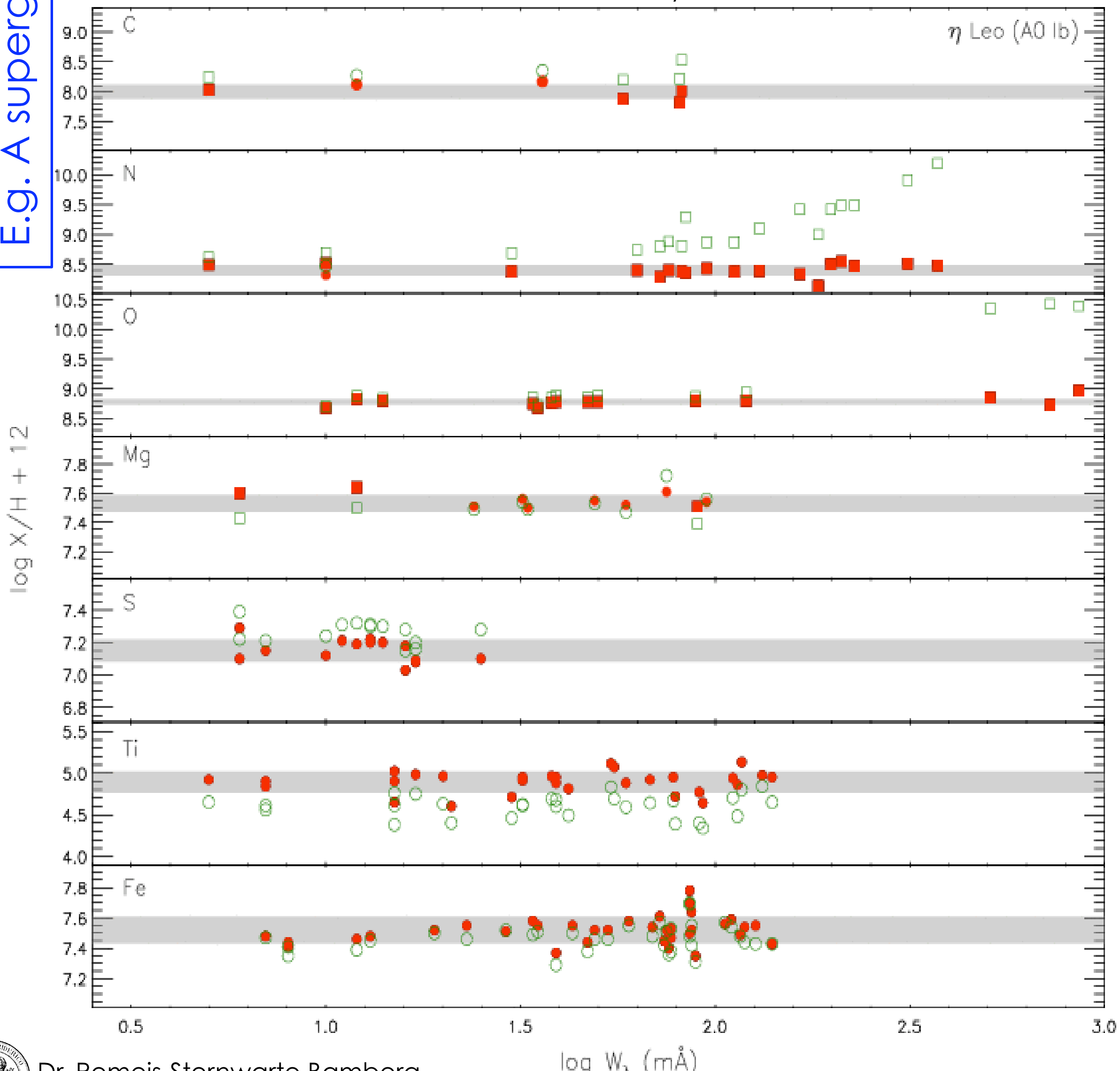

NLTE:
absolute abundances
&
reduced statistical &
systematic uncertainties

Δ log ε :
1σ-stat.: ~ 0.05…0.10 dex
1σ-syst.: ~ 0.07…0.12 dex

typical uncertainties
in literature (LTE): x ~2-3
+ unknown systematic
errors

NLTE/LTE
neutral
ionized

Global Spectrum Synthesis

E.g. A supergiant

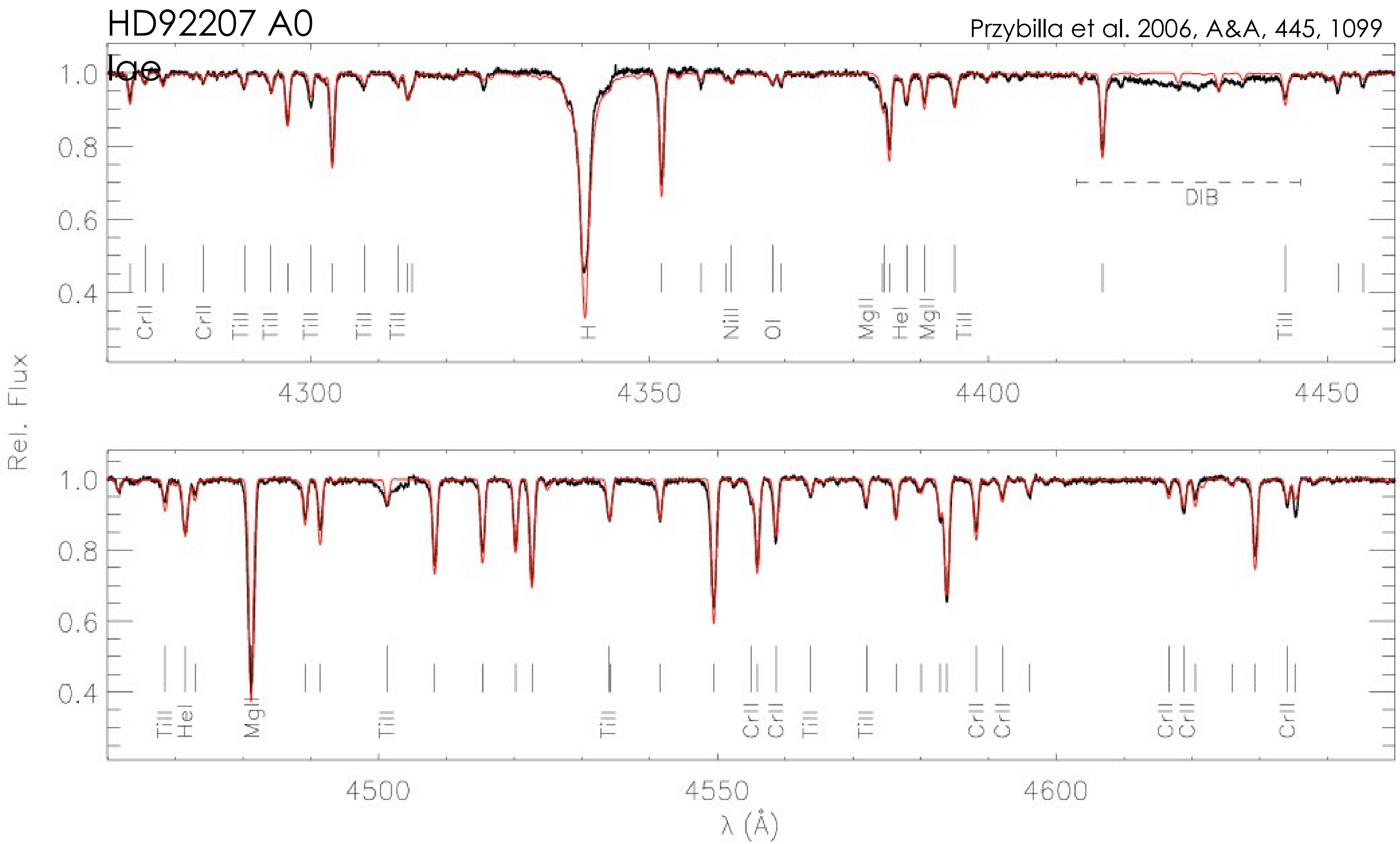

- good agreement may be obtained in global and in detail